

A study on film boiling using a Coupled Level Set and Volume of Fluid (CLSVOF) method for constant temperature and constant heat flux wall models for 2D and Axi-symmetric cases.

Subhrajit Bhattacharya
Dept. of Mechanical Engineering,
IIT Kharagpur.

1. Introduction:

Boiling is an extremely important process having vast application in various fields of science, technology & industries. Despite this, the fundamental mechanisms involved in the process are far from being understood. In the complete phase change problem the mass, momentum and energy transport equations must typically include the effects of surface tension, latent heat, interface mass transfer, discontinuous material properties and complicated liquid-vapour dynamics.

Over the recent years several studies have been made to clarify and model the interface transport mechanism associated with liquid-vapour phase change process, such as film boiling.

In the past several experimental works have been performed for understanding the phenomena of boiling. But those early investigations could not provide suitable physical details needed for understanding bubble formation and the time varying heat transfer characteristics. However experimental studies have resulted in several empirical correlations, which are valid in specific cases.

Hence only suitable computational techniques are the only way by which the investigation can be made in detail. The first successful attempt for solving two phase flows with sharp interfaces was done using the VOF method due to Hirt and Nichols [5]. The VOF method has been successfully implemented by Welch and Wilson [6] for simulation of boiling flows. Juric and Tryggvason [7] implemented a method using an indicator function, similar to VOF, for computation of boiling flows. In this method unified conservation equations are written for the entire flow field and the different phases are treated as one fluid with variable material properties. Similar approach was adopted by Unverdi and Tryggvason [8]. Welch and Rachidi [9] developed another VOF based interface tracking method and successfully implemented it for simulation of film boiling. Agarwal *et al.* [17] used a variant of VOF method for simulation of bubble growth in Film Boiling.

Son and Dhir [10] simulated film boiling on a horizontal surface, solving governing equations for both liquid and vapour phase separately in transformed coordinate system. Banerjee and Dhir [11] used similar approach to study subcooled film boiling. Dhir [12] did a Numerical Simulation of Pool-Boiling Heat Transfer. But the main disadvantage of this method is that it can track the interface as long as there is a single disjoint interface, but fails when there are multiple isolated interfaces. So this method can't predict the interfaces after detachment of a bubble in film boiling.

The Level Set formulation for interface tracking was first introduced by Osher and Sethian [13]. Sussman *et al.* [14] used the Level Set approach to compute solutions to incompressible two-phase flow. Son and Dhir [15] have implemented the Level Set method for numerical simulation of film boiling. Chang *et al.* [4] developed a Level Set formulation for computing incompressible multiphase fluid flows.

But there are advantages and disadvantages of both VOF and Level Set methods. The volume-of-fluid (VOF) method does not give satisfactory result in the normal and curvature calculations at the interface, whereas in the Level Set method the LS function

ϕ being a smooth function is readily used to calculate the normal and curvature at the interface. However the advection of LS function turns out to be inefficient in mass conservation. Hence for advection of mass the void fractions of VOF method is suitable. Hence a Coupled Level Set and Volume of Fluid (CLSVOF) method combining the advantageous parts of both the method was used by Sussman and Puckett in [3].

In the present work the CLSVOF method has been used for computing two-phase flow in the problem of film boiling. The model assumes that the location of bubbles are spaced on a solid surface in a square pattern separated by the Taylor fastest-growing wavelength given by Berenson [2].

$$\lambda_0 = 2\pi \sqrt{\frac{3\sigma}{(\rho_l - \rho_g)g}} \quad (1)$$

The present work is mainly an extension of the work by Agarwal *et al.* [17]. The work of Agarwal *et al.* [17] used VOF method to simulate the film boiling for water at a near-critical point for 2D case. It also included the property variations due to temperature variations in the solution domain. In the present work simulations have been performed using CLSVOF method for R-22 at near critical point. Apart from this simulations have been performed for water at near critical point in axisymmetric case and for constant heat flux through a solid wall. However the property variation has been excluded in the present work.

2. Formulation:

2.1. Governing equations :

The momentum transport equation for incompressible flow in the single-phase regions (i.e. either the vapour or the liquid) is,

$$\rho(\mathbf{U}_t + \nabla \cdot \mathbf{U}\mathbf{U}) = -\nabla p + \rho \mathbf{g} + \nabla \cdot (2\mu \mathbf{D}) \quad (2)$$

And at the interface the modified momentum equation incorporating surface tension force due to Brackbill *et al.* [16] becomes,

$$\rho(\mathbf{U}_t + \nabla \cdot \mathbf{U}\mathbf{U}) = -\nabla p + \rho \mathbf{g} + \nabla \cdot (2\mu \mathbf{D}) + \gamma \kappa \mathbf{n} \quad (3)$$

where \mathbf{n} is the unit normal vector at the interface, κ is the curvature of the interface, and \mathbf{D} is defined as the rate of deformation tensor,

$$\mathbf{D} = (\nabla \mathbf{U}) + (\nabla \mathbf{U})^T \quad (4)$$

The mass conservation equation for the incompressible flow in the single-phase regions,

$$\nabla \cdot \mathbf{U} = 0 \quad (5)$$

The method used to solve for velocity and pressure is a variable density approximate projection method described in [3].

And the energy equation in the single-phase regions is given by,

$$\frac{\partial T}{\partial t} + \mathbf{U} \cdot \nabla T = \frac{k}{\rho c} \nabla^2 T \quad (6)$$

However both the mass conservation equation (5) and the energy equations (6) need to be modified at the interface where there is a jump in mass and energy as discussed in § 2.2.

For the problem with a solid wall below the fluid computational domain, the energy equation for the solid region is given by,

$$\frac{\partial T}{\partial t} = \frac{k_s}{\rho_s c_s} \nabla^2 T \quad (7)$$

2.2. Mass and Energy jump Conditions:

Due to phase change at the interface there is a jump in the mass and energy across the interface.

Considering a computational two-phase cell with a part of the interface, the mass balance equation for each phase in the cell can be written as,

$$\frac{d}{dt} \int_{V_G(t)} \rho dV + \int_{S_G(t)} \rho \mathbf{U} \cdot \mathbf{n} dS + \int_{S_I(t)} \rho (\mathbf{U} - \mathbf{U}_I) \cdot \mathbf{n} dS = 0 \quad (8)$$

$$\frac{d}{dt} \int_{V_L(t)} \rho dV + \int_{S_L(t)} \rho \mathbf{U} \cdot \mathbf{n} dS + \int_{S_I(t)} \rho (\mathbf{U} - \mathbf{U}_I) \cdot \mathbf{n} dS = 0 \quad (9)$$

where, $V_L(t)$, $S_L(t)$, $V_G(t)$ and $S_G(t)$ are the volumes and surface area of the cell boundary at the liquid region and the vapour region respectively. $S_I(t)$ is the phase interface at the common boundary of the two regions moving with velocity \mathbf{U}_I . The unit normal vector \mathbf{n} points into the liquid phase on S_I .

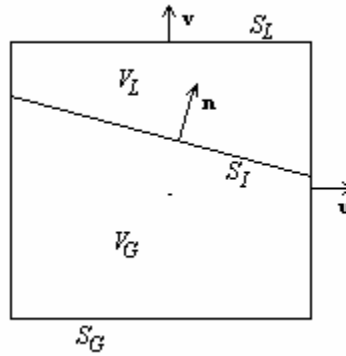


Figure 1

From the above equations and taking into account the incompressibility of each phase, and that the total volume of the cell remains time invariant, the conservation of mass equation for the cell is given by,

$$\int_{S_C} \mathbf{U} \cdot \mathbf{n} dS + \int_{S_I(t)} \|(\mathbf{U} - \mathbf{U}_I)\| \cdot \mathbf{n} dS = 0 \quad (10)$$

Here $\| \cdot \|$ indicates the jump in the variable across the interface and S_C is the boundary of the computational cell.

The mass jump condition at the interface is,

$$\| \rho (\mathbf{U} - \mathbf{U}_I) \| \cdot \mathbf{n} = 0 \quad (11)$$

Similarly the energy jump condition is,

$$\| \rho h (\mathbf{U} - \mathbf{U}_I) \| \cdot \mathbf{n} = - \| \mathbf{q} \| \cdot \mathbf{n} \quad (12)$$

where \mathbf{q} is the heat flux vector at the interface and h is the enthalpy.

From (11) and (12) the jump in the conservation of mass equation becomes,

$$\|(\mathbf{U} - \mathbf{U}_I)\| \cdot \mathbf{n} = \left(\frac{1}{\rho_l} - \frac{1}{\rho_g} \right) \frac{\| \mathbf{q} \| \cdot \mathbf{n}}{h_{lg}} \quad (13)$$

Using (10) and (13) we have the continuity equation at the interface as,

$$\int_{S_C} \mathbf{U} \cdot \mathbf{n} dS + \int_{S_I(t)} \left(\frac{1}{\rho_l} - \frac{1}{\rho_g} \right) \frac{\| \mathbf{q} \| \cdot \mathbf{n}}{h_{lg}} \cdot \mathbf{n} dS = 0 \quad (14)$$

2.3. Interface tracking using The Level Set function:

In the LS method a smooth function ϕ is used to represent the interface. The function $\phi(\mathbf{r}, t)$ at a point with position vector \mathbf{r} and at a time instant t assumes values as follows:

$$\phi(\mathbf{r}, t) \begin{cases} < 0 & \text{in gas region} \\ = 0 & \text{at the interface} \\ > 0 & \text{in liquid region} \end{cases}$$

The level set function chosen here is maintained as the signed distance from the interface close to the interface. Hence, near the interface,

$$\phi(\mathbf{r}, t) \begin{cases} = -d & \text{in gas region} \\ = 0 & \text{at the interface} \\ = +d & \text{in liquid region} \end{cases} \quad (15)$$

where $d = d(t)$ is the shortest distance of the interface from point \mathbf{r} .

From such a representation of the interface, the unit normal vector \mathbf{n} and the mean curvature κ are simply,

$$\mathbf{n} = \frac{\nabla \phi}{|\nabla \phi|} \quad (16)$$

and,

$$\kappa = -\nabla \cdot \frac{\nabla \phi}{|\nabla \phi|} \quad (17)$$

On the other hand, the LS method has the disadvantage that the discretizations of the equation to advect level set function (19) is prone to more numerical errors than front tracking method or VOF method, specially when the interface experiences severe stretching or tearing.

2.3. Modified Equations:

Using the level set formulation due to Chang *et al.* [4], the momentum transport equation for incompressible two-phase flow becomes,

$$\rho(\phi) (\mathbf{U}_t + \nabla \cdot \mathbf{U}\mathbf{U}) = -\nabla p + \rho(\phi) \mathbf{g} + \nabla \cdot (2\mu(\phi) \mathbf{D}) + \gamma \kappa(\phi) \nabla H(\phi) \quad (18)$$

and the LS function advection equation is,

$$\frac{\partial \phi}{\partial t} + \mathbf{U} \cdot \nabla \phi = 0 \quad (19)$$

where H is the Heaviside function,

$$H(\phi) = \begin{cases} 1 & \text{if } \phi > 0 \\ 0 & \text{otherwise} \end{cases} \quad (20)$$

and \mathbf{D} is defined as the rate of deformation tensor given by (4),
And the density (ρ) and viscosity (μ) are given by,

$$\rho(\phi) = \rho_g(1 - H(\phi)) + \rho_l H(\phi) \quad (21)$$

$$\mu(\phi) = \mu_g(1 - H(\phi)) + \mu_l H(\phi) \quad (22)$$

where, H is the Heaviside function given by (20), and the curvature κ is given by (16).

When discretizing the level set equation (19), the volume-of-fluid function F is also simultaneously solved from the following equation,

$$\frac{\partial F}{\partial t} + \nabla \cdot (\mathbf{U}F) = 0 \quad (23)$$

3. Numerical Methods and Discretizations:

3.1. Discretization of Momentum and Continuity Equation :

The momentum equation (18) is discretized using a first order scheme as,

$$\mathbf{U}^{n+1} = \mathbf{U}^n + \left(-\nabla \cdot \mathbf{U}^n \mathbf{U}^n + \mathbf{g} + \frac{-\nabla p^{n+1} + \nabla \cdot (2\mu(\phi^n) \mathbf{D}) + \gamma \kappa(\phi^n) \nabla H(\phi^n)}{\rho(\phi^n)} \right) \delta t \quad (24)$$

The convection term for the incompressible flow is discretized using a High-Order upwind ENO scheme as described in [4].

The continuity equation in the single-phase regions (5) and at the interface (14) are respectively discretized as follows,

$$\nabla \mathbf{U}^{n+1} = 0 \quad (25)$$

and,

$$\int_{S_c} \mathbf{U}^{n+1} \cdot \mathbf{n} dS + \int_{S_f(t)} \left(\frac{1}{\rho_l} - \frac{1}{\rho_g} \right) \frac{\|\mathbf{q}^{n+1}\| \cdot \mathbf{n}}{h_{lg}} \cdot \mathbf{n} dS = 0 \quad (26)$$

For solving the pressure, the pressure correction is done using a variable density approximate projection method described in [3].

3.2. Discretization of Energy Equation :

In the vapour region the Energy Equation (6) is solved using an implicit scheme,

$$T^{n+1} = T^n + \left(-\mathbf{U} \cdot \nabla T^{n+1} + \frac{k}{\rho c} \nabla^2 T^{n+1} \right) \delta t \quad (27)$$

However in the liquid region and at the interface the temperature is taken to be constant at the saturation temperature. Hence in the liquid and at the interface,

$$T = T_{sat} \quad (28)$$

In the solid region the Energy Equation (7) is solved using an implicit scheme,

$$T^{n+1} = T^n + \left(\frac{k_s}{\rho_s c_s} \nabla^2 T^{n+1} \right) \delta t \quad (29)$$

3.3. The CLSVOF advection algorithm :

A coupled second order conservative operator split advection scheme was used for discretizations of (19) and (23) as described in [3]. At each time step after finding the updated level set function ϕ^{n+1} and the volume-of-fluid function F^{n+1} , the level set function ϕ is reinitialised to the exact signed normal distance to the reconstructed interface by “coupling” the level set function to the volume fraction. The algorithm used for this is that given in [3].

3.4. Calculation of Curvature for 2D and axisymmetric case :

The normal as given by (16) has same expression for both 2D and axisymmetric case,

$$\mathbf{n} = \frac{\phi_r \mathbf{i} + \phi_z \mathbf{j}}{\sqrt{\phi_r^2 + \phi_z^2}} \quad (30)$$

where, \mathbf{i} and \mathbf{j} are the unit vectors along the two orthogonal reference axes.

The curvature in (17) is given by,

$$\kappa = - \left(\frac{\phi_z^2 \phi_{rr} - 2\phi_r \phi_z \phi_{rz} + \phi_r^2 \phi_{zz}}{(\phi_r^2 + \phi_z^2)^{3/2}} + \xi \frac{1}{r} \frac{\phi_r}{\sqrt{\phi_r^2 + \phi_z^2}} \right) \quad (31)$$

where, $\xi = 0$ for 2D case, and $\xi = 1$ for axisymmetric case.

4. Boundary Conditions :

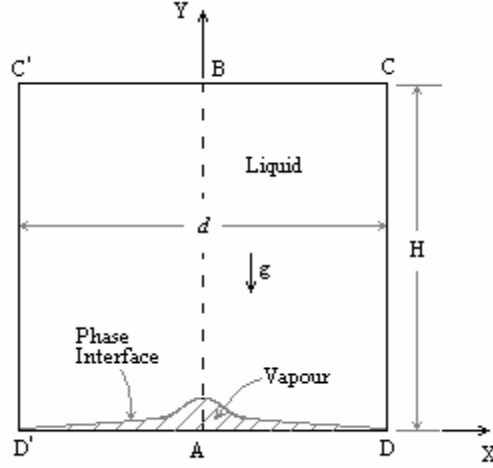


Figure 2

Figure 2 shows the domain of interest for the present problem. The computational domain is ABCD with width $d/2$ and height H . The value of H was chosen suitably for the different cases. The value of d was taken to be λ_0 for 2D case and $\lambda_0/\sqrt{2}$ for axisymmetric case.

AB is the axis of symmetry in the 2D case and is the axis for rotation in axisymmetric case. In either of the cases AB is an axis of mirror symmetry. Hence the boundary condition along AB (i.e. $x=0$) is,

$$\text{at } x=0: \quad u=0, \frac{\partial v}{\partial x}=0, \frac{\partial T}{\partial x}=0, \frac{\partial F}{\partial x}=0, \frac{\partial \phi}{\partial x}=0$$

CD is also an axis of symmetry in 2D case. In axisymmetric case, which is actually an approximation of the 3D case, the line CD is nothing but a plane of symmetry. Hence similar boundary conditions apply along CD,

$$\text{at } x=d/2: \quad u=0, \frac{\partial v}{\partial x}=0, \frac{\partial T}{\partial x}=0, \frac{\partial F}{\partial x}=0, \frac{\partial \phi}{\partial x}=0$$

Outflow boundary conditions are used on the top surface of the domain,

$$\text{at } y=H: \quad \frac{\partial u}{\partial y} = \frac{\partial v}{\partial y} = \frac{\partial T}{\partial y} = \frac{\partial F}{\partial y} = \frac{\partial \phi}{\partial y} = 0; \quad P = P_0$$

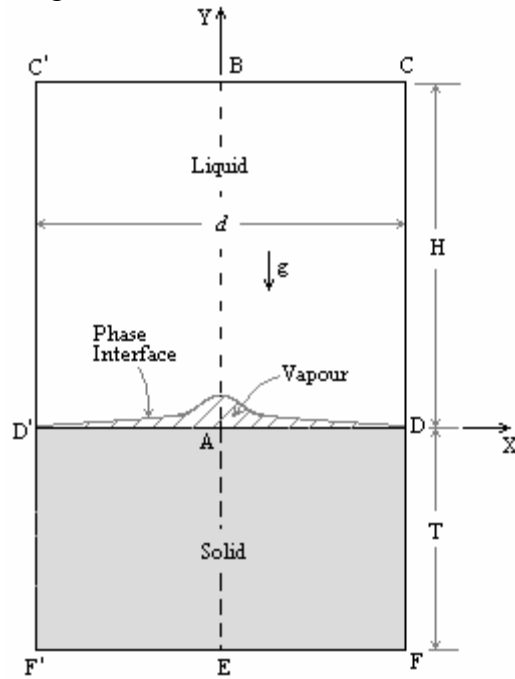
The outlet pressure is taken to be the saturation pressure less than the hydrostatic pressure difference from the initial film level to the outlet.

At the wall AD, two wall-models were used:

For constant wall temperature model,

$$\text{at } y=0: \quad T=T_{sup}$$

For constant heat flux through a solid model:



Below the wall AD a solid region AEFD & AEF'D' was taken. The boundary condition of constant heat flux was applied at the bottom of the solid (i.e. the boundary along EF).

5. Results :

5.1. Case-1 : R-22 at near critical-point :

Refrigerant-22 being an important fluid having application in various industrial and scientific fields is an interesting fluid chosen for study.

At the interface the following near-critical fluid properties are used:

$$T_{sat} = 355 \text{ K}; \quad P_{sat} = 3800 \text{ KPa}; \quad h_{lg} = 95.7 \text{ KJ/Kg}; \quad \sigma = 1 \text{ mN/m}$$

The following properties are used for the liquid and vapour phase:

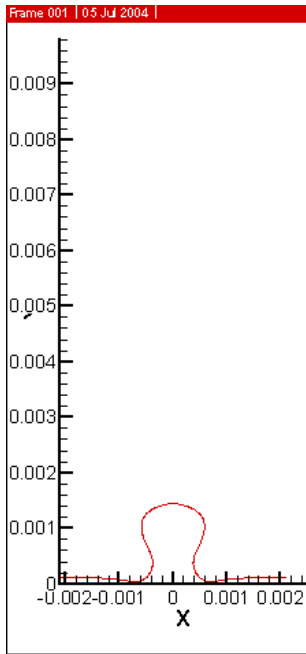
| | Density(ρ) (Kg/m ³) | Viscosity(μ) ($\mu\text{N s/m}^2$) | Conductivity(k) (mW/m K) | Specific Heat(c_p) (KJ/Kg K) |
|--------|---|---|---------------------------------|-------------------------------------|
| Liquid | 887 | 119 | 44 | 2.43 |
| Vapour | 208 | 18.8 | 18.8 | 2.31 |

The domain size is chosen to be $\frac{\lambda_0}{2} \times \frac{5}{2}\lambda_0$, i.e. $d = \lambda_0$ and $H = \frac{5}{2}\lambda_0$. Grid resolution chosen was 100×500 . The grids were taken to be uniform square grids.

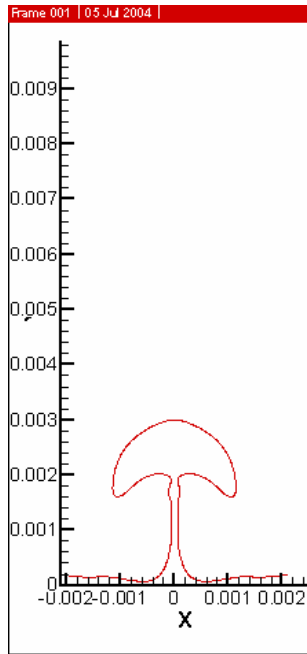
The solution was done for a 2D case.

The wall model was chosen to be a constant temperature one with $\Delta T = 15 \text{ K}$, i.e. $T_{sup} = 370 \text{ K}$.

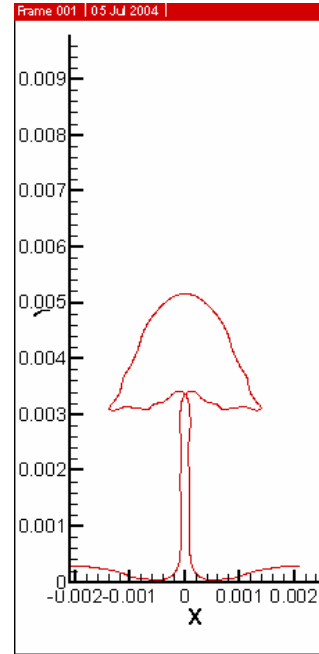
The R-22 bubble profile at various time steps captured in the solution domain:



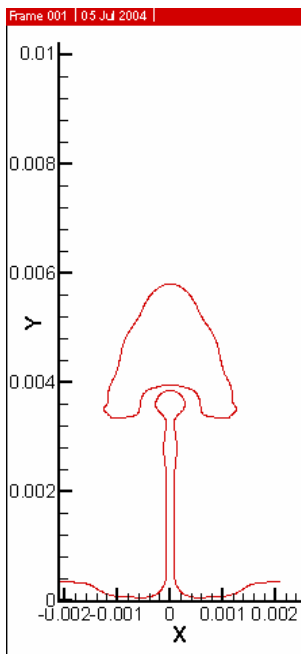
$t = 0.06\text{s}$



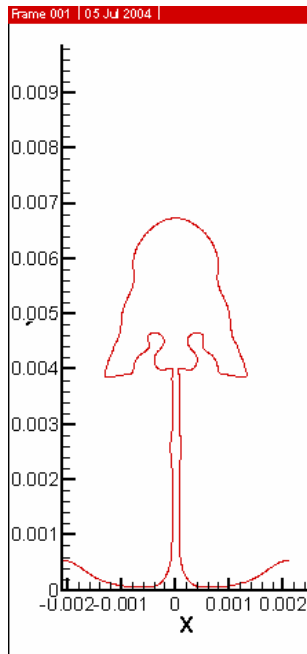
$t = 0.08\text{s}$



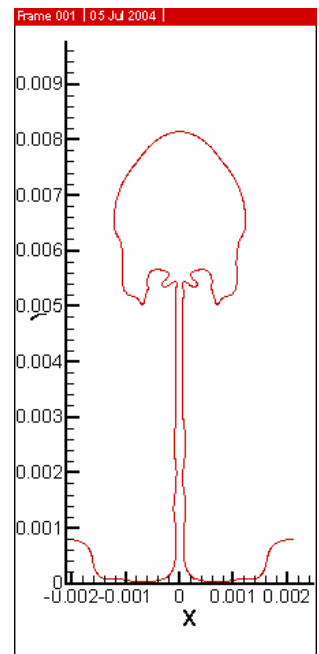
$t = 0.10\text{s}$



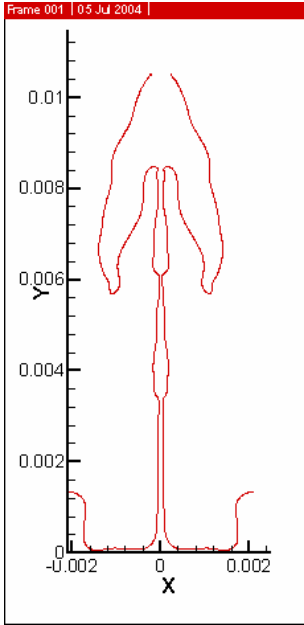
$t = 0.10385\text{s}$



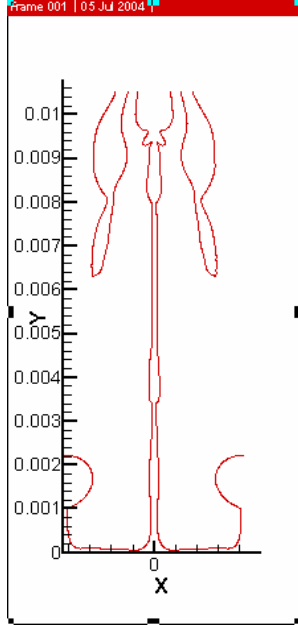
$t = 0.11070\text{s}$



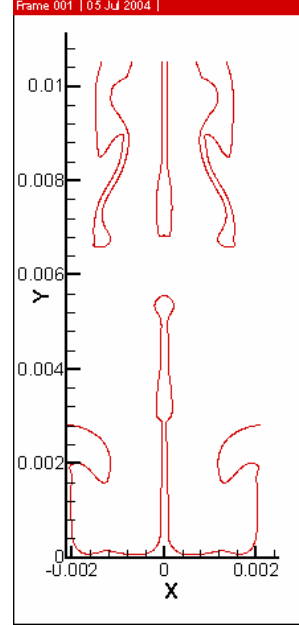
$t = 0.12\text{s}$



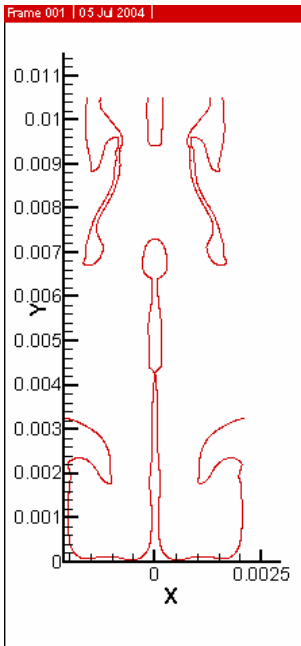
$t = 0.13s$



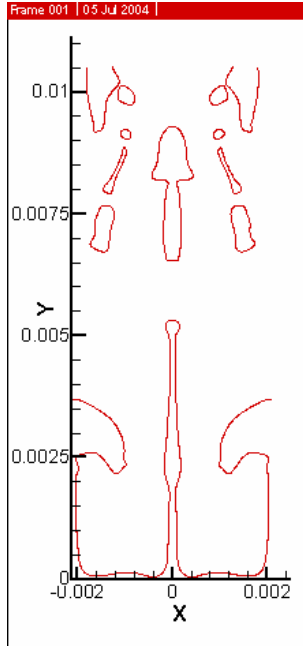
$t = 0.14325s$



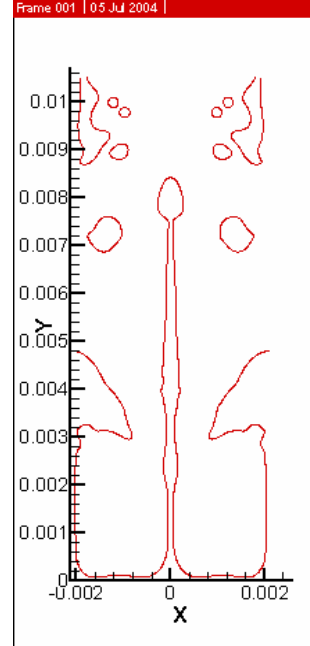
$t = 0.15s$



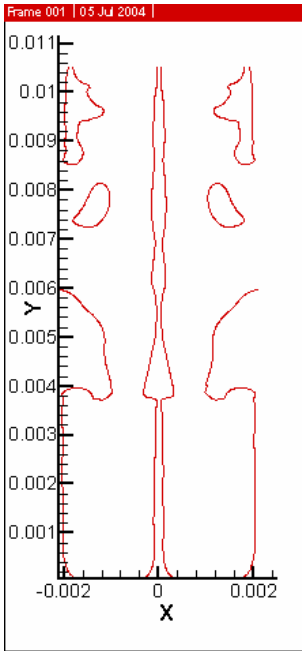
$t = 0.155s$



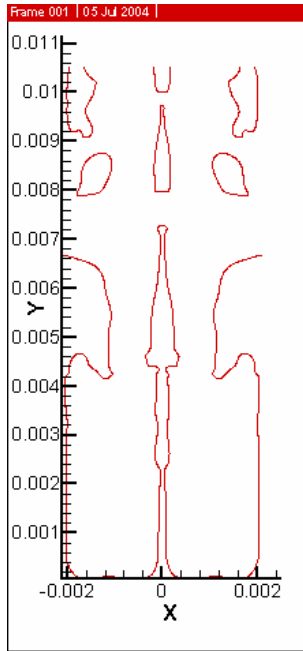
$t = 0.16s$



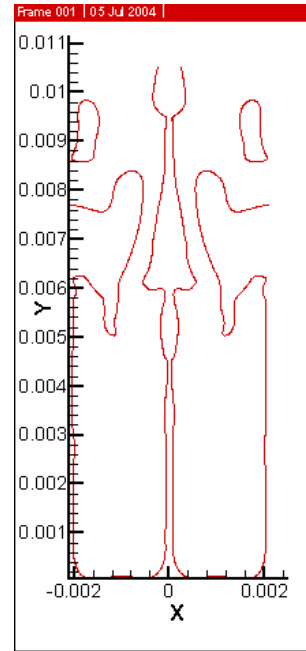
$t = 0.17s$



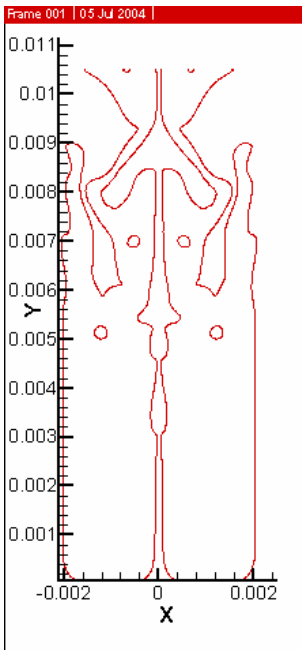
$t = 0.18\text{s}$



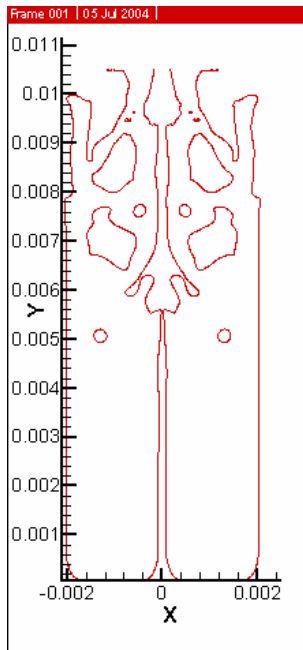
$t = 0.18565\text{s}$



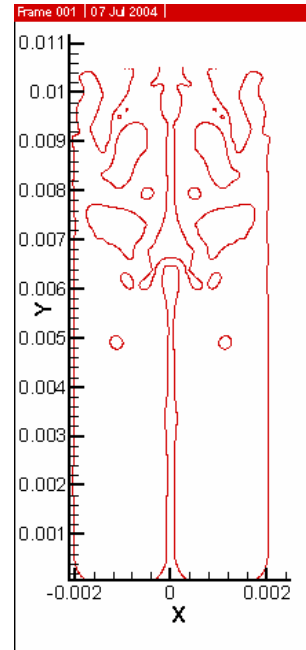
$t = 0.2\text{s}$



$t = 0.22\text{s}$

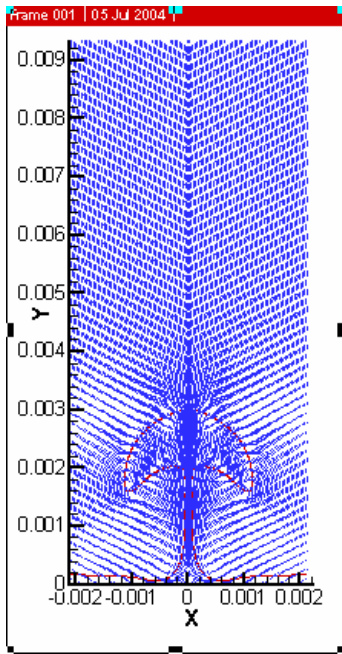


$t = 0.22665\text{s}$

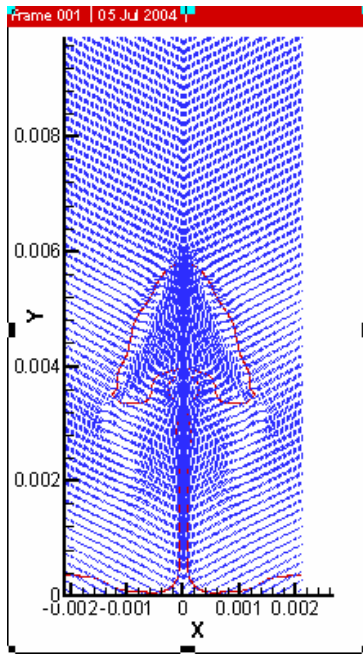


$t = 0.23\text{s}$

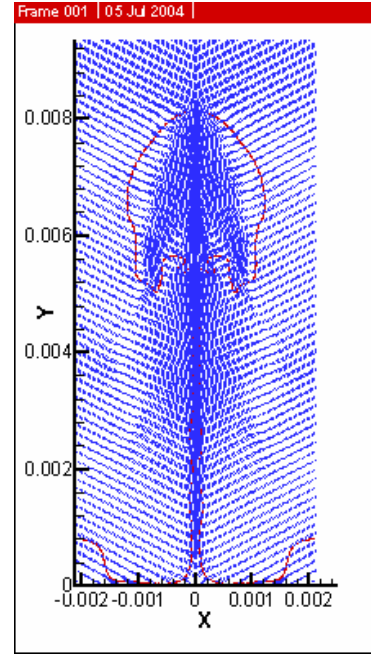
Velocity vector field at some time steps:



$t = 0.08\text{s}$

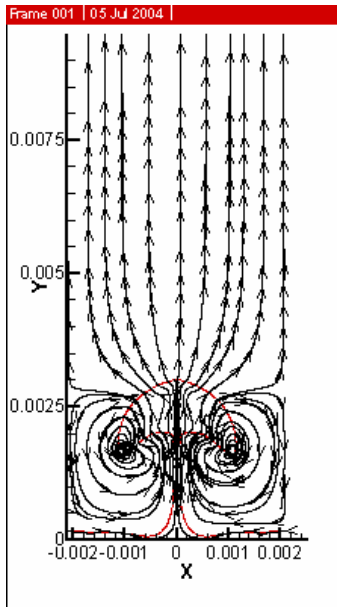


$t = 0.10385\text{s}$

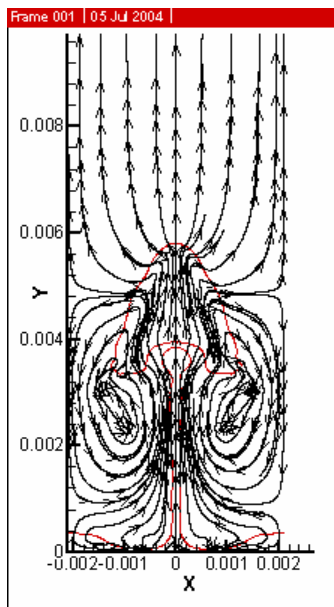


$t = 0.12000\text{s}$

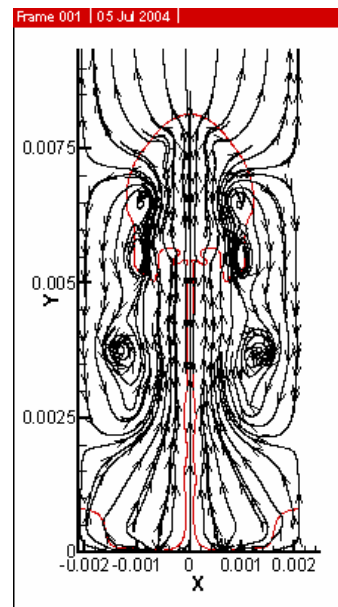
Streamlines at some time steps:



$t = 0.08\text{s}$

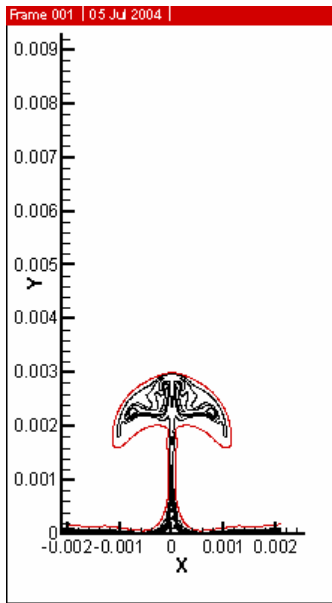


$t = 0.10385\text{s}$

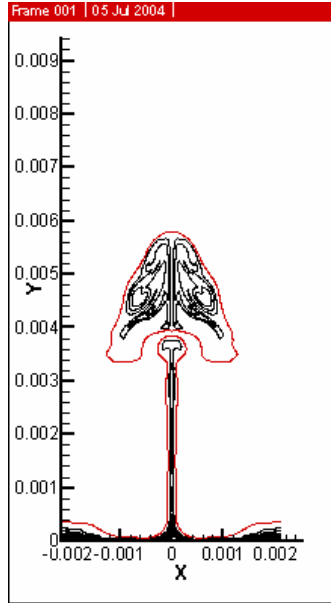


$t = 0.12\text{s}$

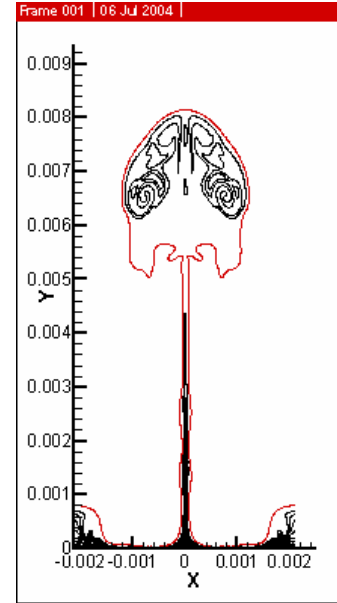
Temperature contours at some time steps:



$t = 0.08\text{s}$

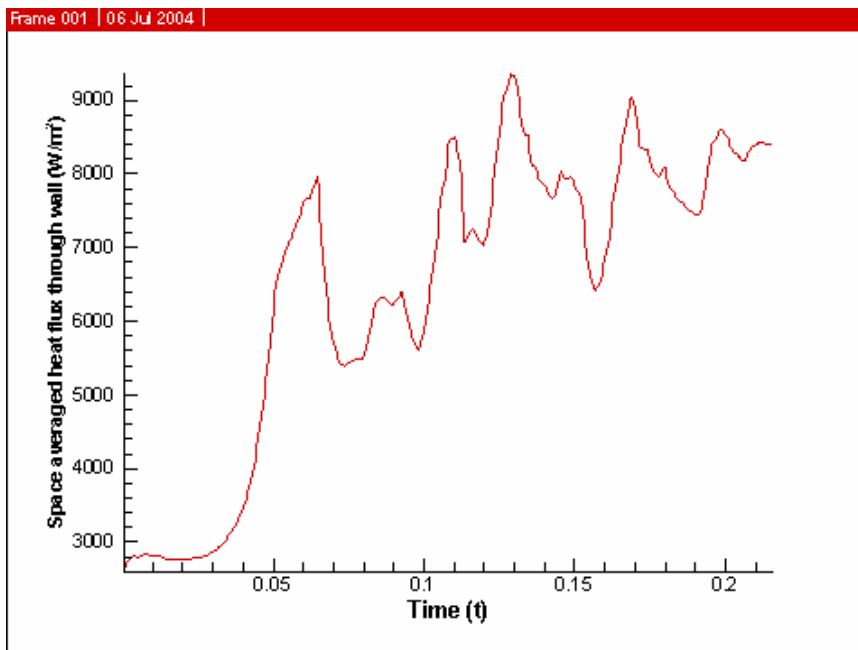


$t = 0.10385\text{s}$



$t = 0.12\text{s}$

Space-averaged heat flux through wall:



It is observed that the bubble growth takes place till about $t=0.1$ s. Then at around $t=0.103$ s the bubble detaches from the stem. However it reattaches with the stem very soon at $t=0.11$ s. This phenomena may be attributed to the notably low value of h_{lg} of R-22 at near critical point. This low value leads to rapid formation of vapour and hence a relatively higher rate of elongation of vapour stem than the rate in which the detached bubble escapes. This hence causes the reattachment of the bubble with the vapour stem.

The formation of the long vapour stem and simultaneous formation of bubbles at nodes and antinodes are observed. This may probably due to the comparatively high value of surface tension, which prevents the bubble from detaching the main vapour stem completely. Probably that is also the reason behind the formation of small bubbles and their further breaking down into smaller bubbles in order to reduce the high surface energy.

In between $t=0.06$ s and $t=0.08$ s, necking started to take place. This phenomena was clearly reflected in the graph of space averaged heat flux through wall in which a sudden shoot-up and a consecutive sudden fall in the flux was observed.

5.2. Case 2 : R-12 at near critical point :

Refrigerant-12 also being an important fluid having application in various industrial and scientific fields is an interesting fluid chosen for study.

At the interface the following near-critical fluid properties are used:

$$T_{sat} = 365 \text{ K}; \quad P_{sat} = 2907 \text{ KPa}; \quad h_{lg} = 75.8 \text{ KJ/Kg}; \quad \sigma = 1.3 \text{ mN/m}$$

The following properties are used for the liquid and vapour phase:

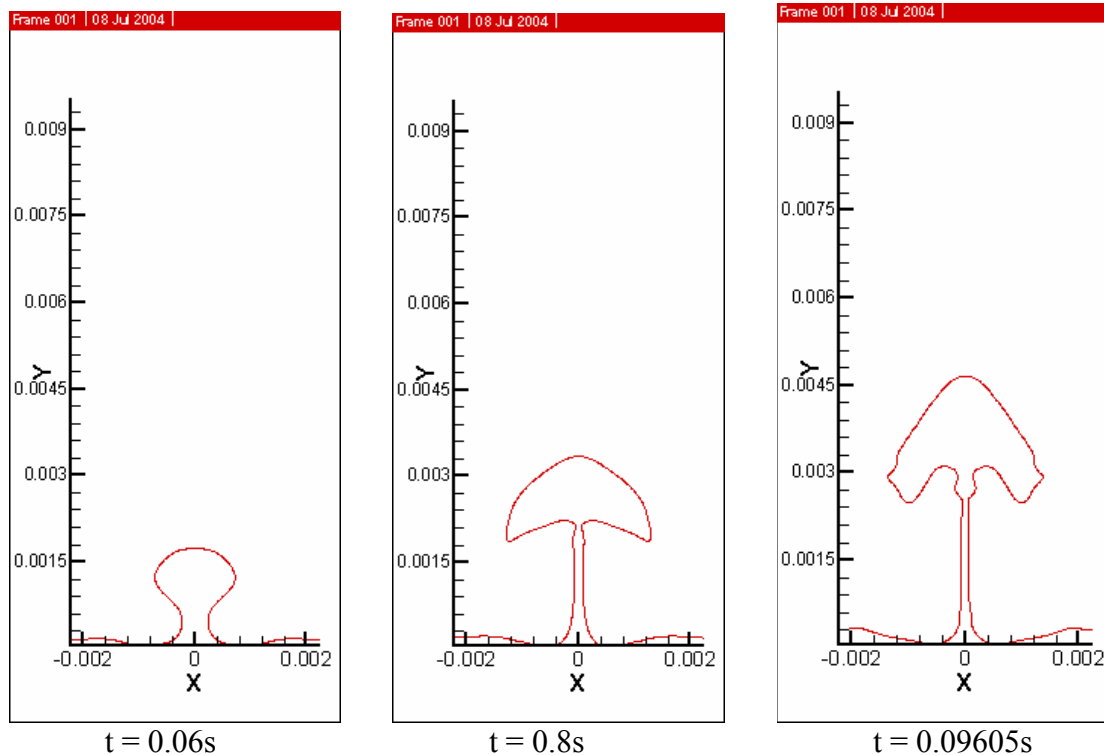
| | Density(ρ) (Kg/m ³) | Viscosity(μ) ($\mu\text{N s/m}^2$) | Conductivity(k) (mW/m K) | Specific Heat(c_p) (KJ/Kg K) |
|--------|---|---|---------------------------------|-------------------------------------|
| Liquid | 969.7 | 119 | 119 | 1.22 |
| Vapour | 203.2 | 18.8 | 18.1 | 1.68 |

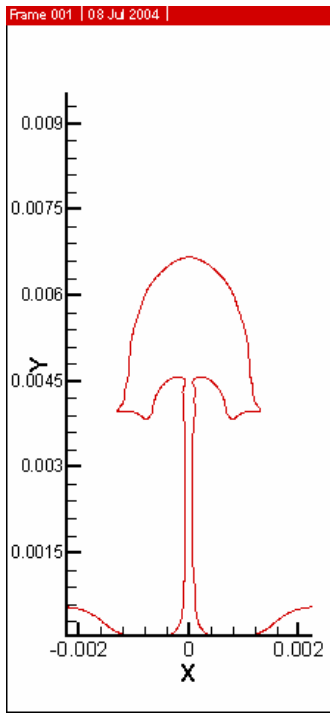
The domain size is chosen to be $\frac{\lambda_0}{2} \times \frac{5}{2}\lambda_0$, i.e. $d = \lambda_0$ and $H = \frac{5}{2}\lambda_0$. Grid resolution chosen was 100×500 . The grids were taken to be uniform square grids.

The solution was done for a 2D case.

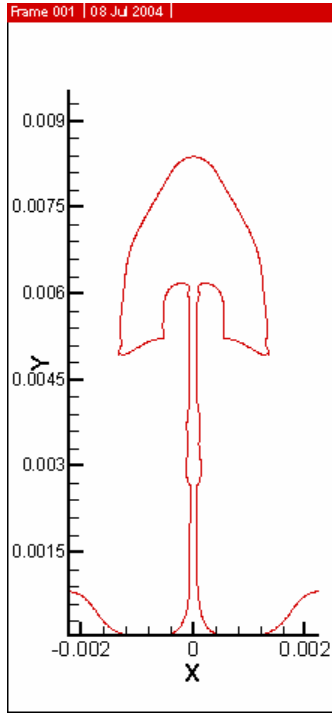
The wall model was chosen to be a constant temperature one with $\Delta T = 15 \text{ K}$, i.e. $T_{sup} = 380 \text{ K}$.

Bubble profile at various time-steps:

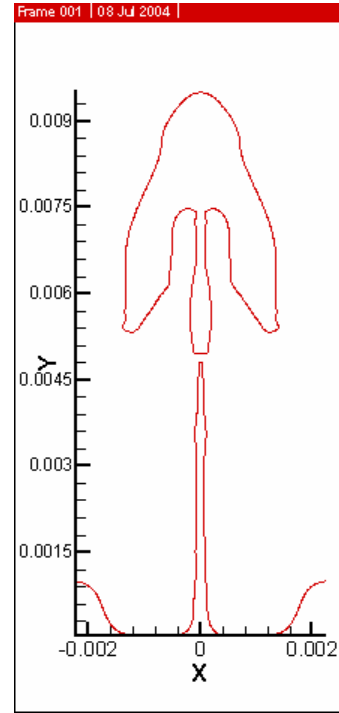




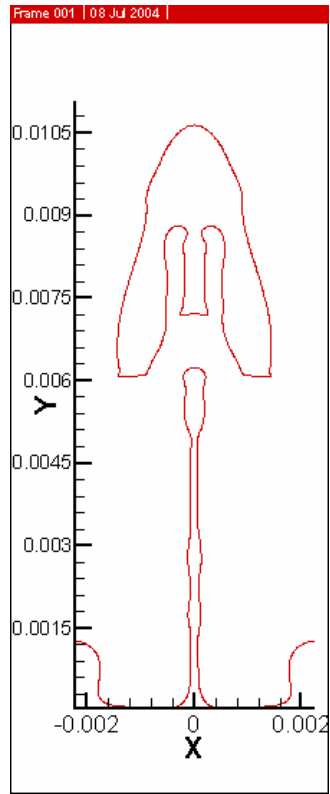
t = 0.1055



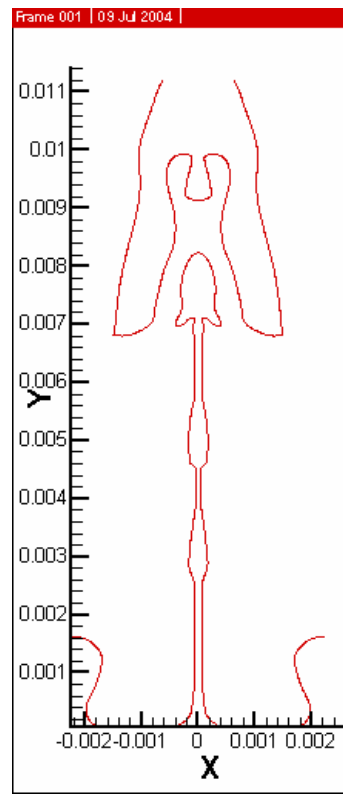
t = 0.115



t = 0.12s

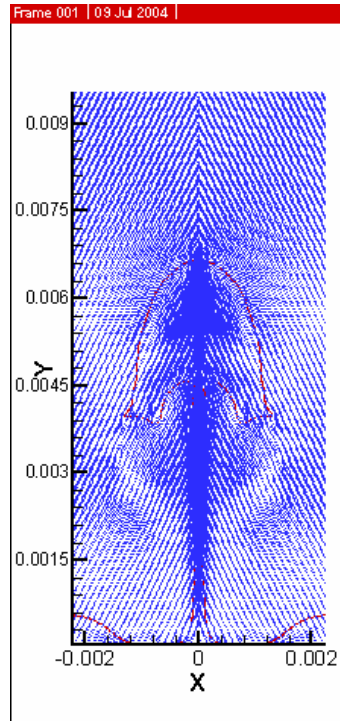


t = 0.125s

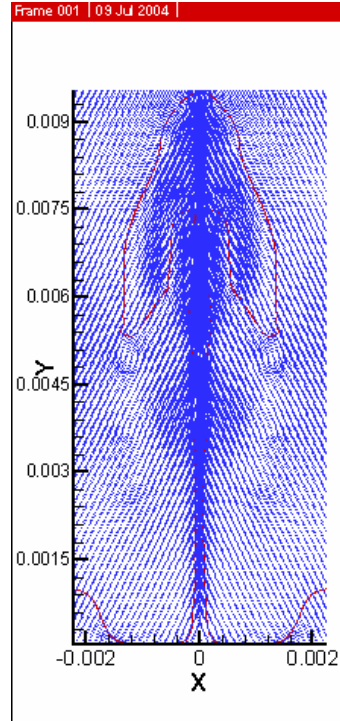


t = 0.13s

Velocity Vector field at some time-steps:

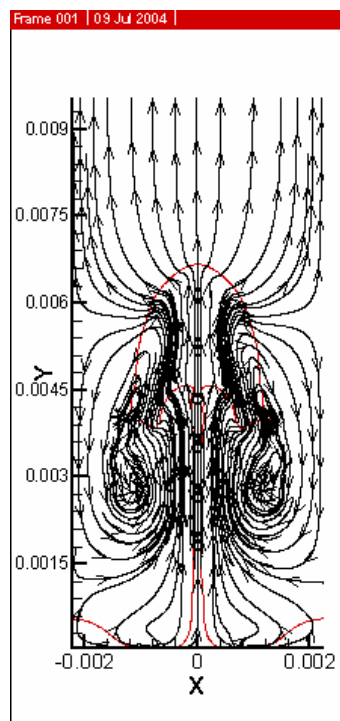


$t = 0.1055\text{s}$

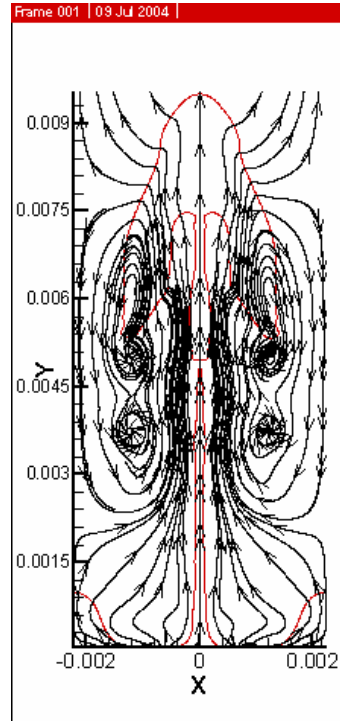


$t = 0.12\text{s}$

Streamlines at some time-steps:

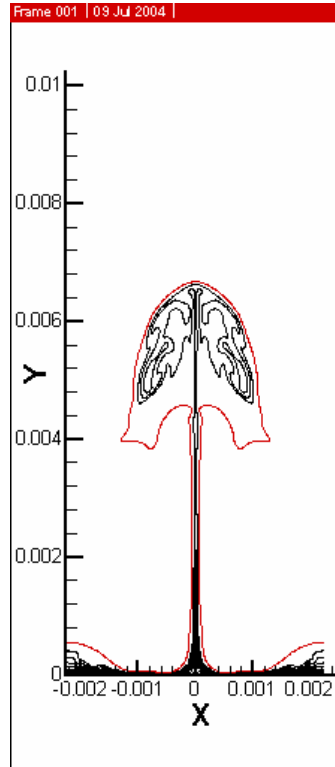


$t = 0.1055\text{s}$

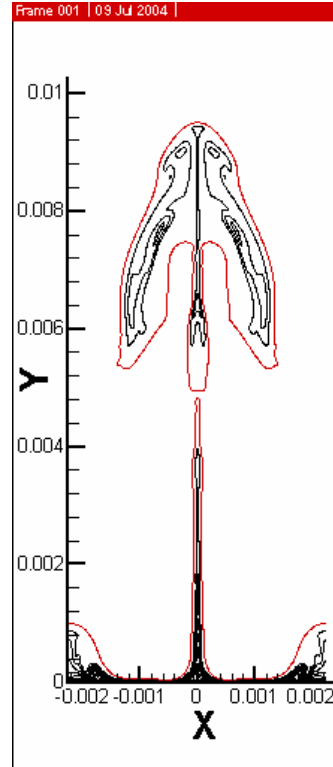


$t = 0.12\text{s}$

Temperature contours at some time-steps:

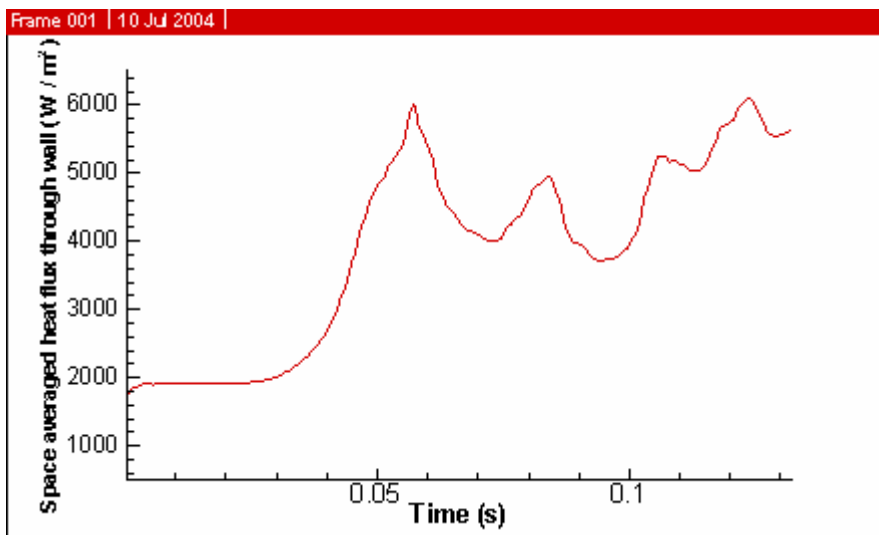


t = 0.1055s



t = 0.12s

Space averaged heat flux through wall:



Almost similar to the formation of the R-22 bubble, in the case of R-12 a long stem of vapour is observed. However the phenomena of reattachment of bubble with stem was not seen till $t=1.3s$.

5.3. Case-3 : Water at near-critical point :

Simulation similar to Section 5.1 or 5.2. was performed using water at near critical point as the fluid. The work of Agarwal *et al.* [17] was done using VOF approach. In the present work CLSVOF has been implemented. The fluid used is water at neat-critical point.

At the interface the following near-critical fluid properties are used:

$$T_{sat} = 646.15 \text{ K}; \quad P_{sat} = 94600 \text{ KPa}; \quad h_{lg} = 276.4 \times 10^4 \text{ KJ/Kg}; \quad \sigma = 0.07 \text{ mN/m}$$

The following properties are used for the liquid and vapour phase:

| | Density(ρ) (Kg/m ³) | Viscosity(μ) ($\mu\text{N s/m}^2$) | Conductivity(k) (mW/m K) | Specific Heat(c_p) (KJ/Kg K) |
|--------|---|---|---------------------------------|-------------------------------------|
| Liquid | 402.4 | 46.7 | 545.4 | 218.28 |
| Vapour | 242.7 | 32.38 | 538.3 | 352.27 |

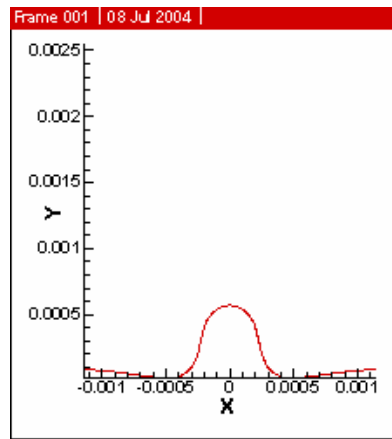
The fluid solution domain size is chosen to be $\frac{\lambda_0}{2} \times 2\lambda_0$, i.e. $H=2\lambda_0$. Grid resolution chosen was 100×400 . The grids were taken to be uniform square grids.

The solution was done for a 2D case.

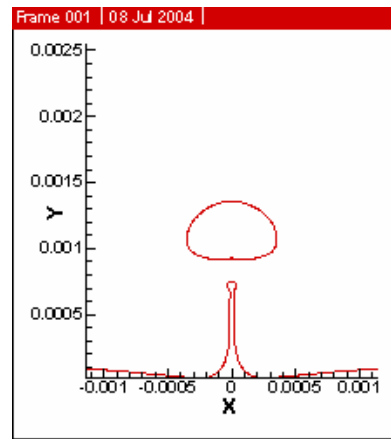
The wall model was chosen to be a constant temperature one with $\Delta T = 15 \text{ K}$, i.e. $T_{sup} = 661.15 \text{ K}$.

Bubble profile at different time-steps:

First half-cycle:

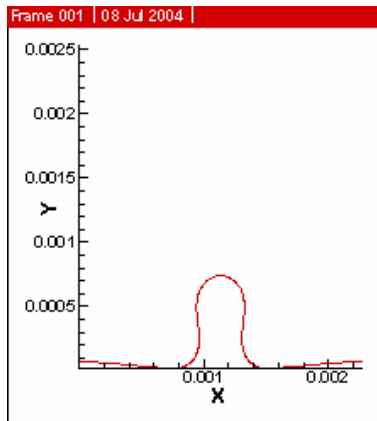


$t = 0.25\text{s}$

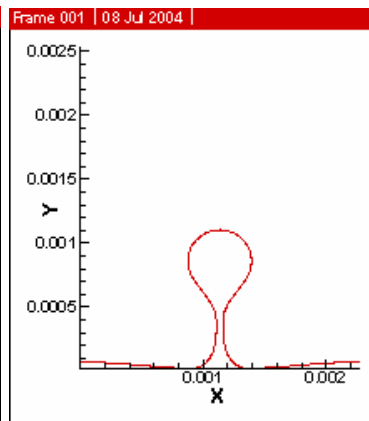


$t = 0.3\text{s}$

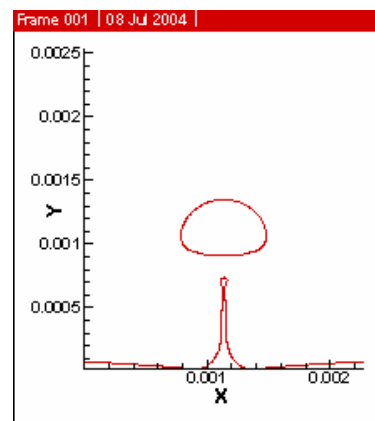
Second half-cycle:



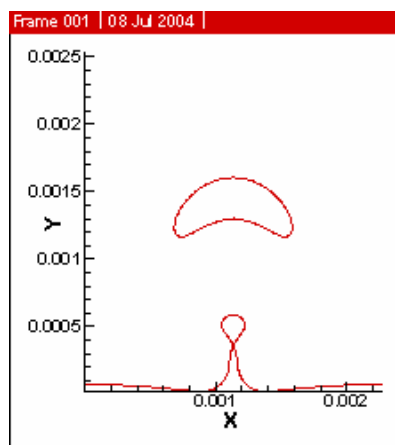
$t = 0.52\text{s}$



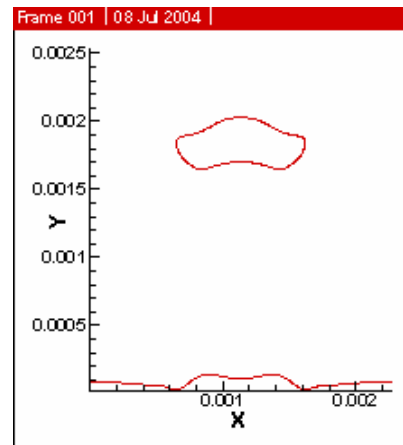
$t = 0.54\text{s}$



$t = 0.55\text{s}$

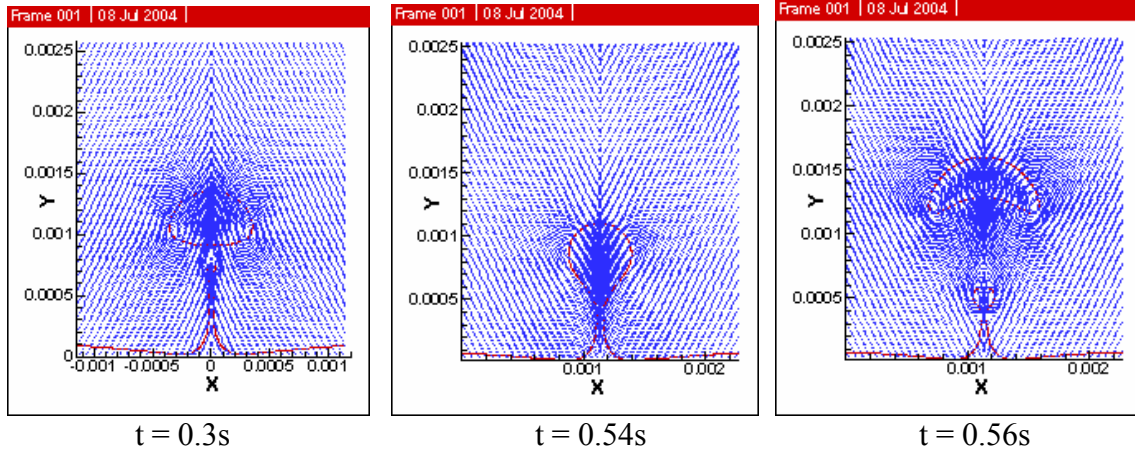


$t = 0.56\text{s}$

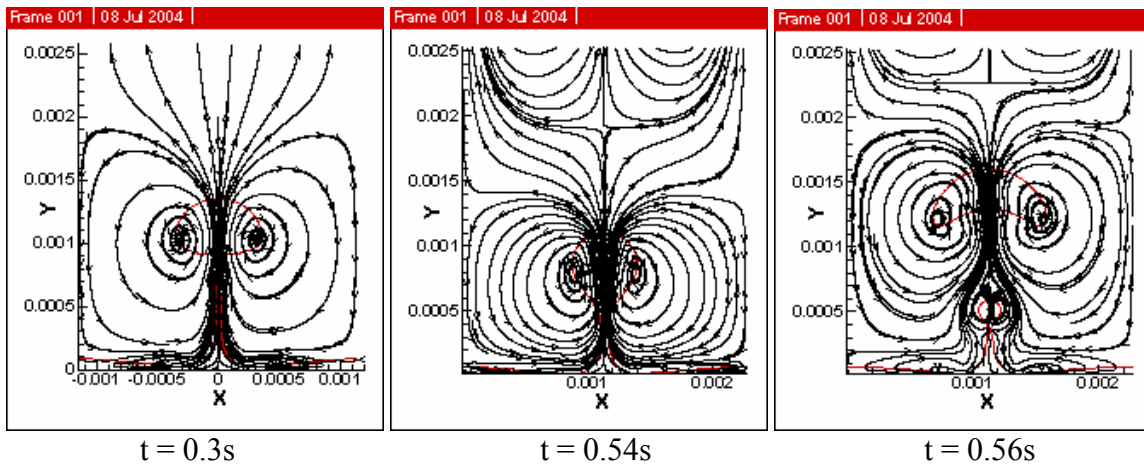


$t = 0.58\text{s}$

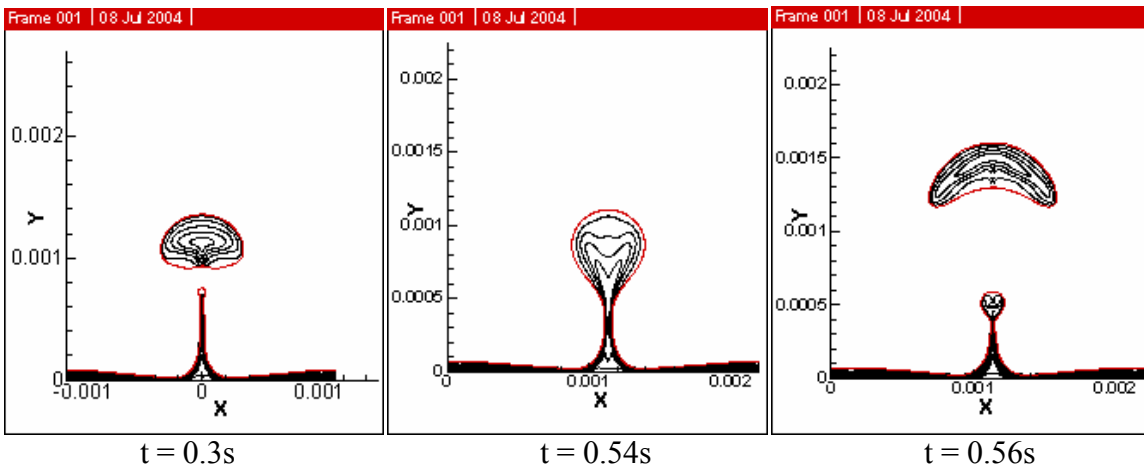
Velocity vector field at some time-steps:



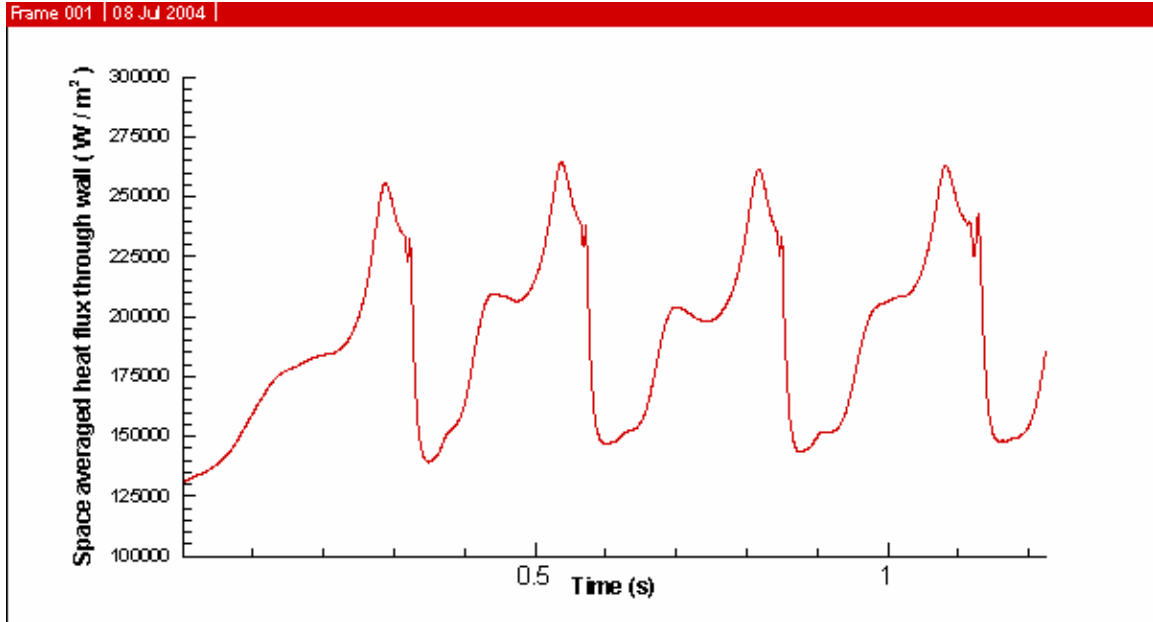
Stream-lines at some time-steps:



Temperature contours at some time-steps:



Space averaged heat flux through wall:



The results obtained in this case were almost similar to those of Agarwal *et al.* [17]. periodic formation of bubbles alternately at nodes and antinodes were observed. The space averaged heat flux through wall was also found to have a periodic nature.

5.4. Case-4 : Constant heat flux through a solid :

The constant wall temperature model used in 5.3 was changed to constant heat flux through a solid. The fluid chosen was water at near-critical conditions.

At the interface the following near-critical fluid properties are used:

$$T_{sat} = 646.15 \text{ K}; \quad P_{sat} = 94600 \text{ KPa}; \quad h_{lg} = 276.4 \times 10^4 \text{ KJ/Kg}; \quad \sigma = 0.07 \text{ mN/m}$$

The following properties are used for the liquid and vapour phase:

| | Density(ρ) (Kg/m ³) | Viscosity(μ) ($\mu\text{N s/m}^2$) | Conductivity(k) (mW/m K) | Specific Heat(c_p) (KJ/Kg K) |
|--------|---|---|---------------------------------|-------------------------------------|
| Liquid | 402.4 | 46.7 | 545.4 | 218.28 |
| Vapour | 242.7 | 32.38 | 538.3 | 352.27 |

The fluid solution domain size is chosen to be $\frac{\lambda_0}{2} \times \lambda_0$, i.e. $d = \lambda_0$ and $H = \lambda_0$. Grid resolution chosen was 100×200 . The grids were taken to be uniform square grids.

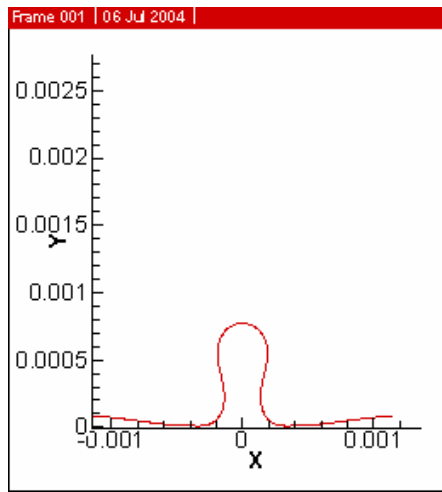
The solid domain size was chosen to be $\frac{\lambda_0}{2} \times \frac{3}{5} \lambda_0$, i.e. $T = \frac{3}{5} \lambda_0$. Grid resolution chosen was 100×120 . The grids in solid were also taken to be uniform square grids.

The solution was done for a 2D case.

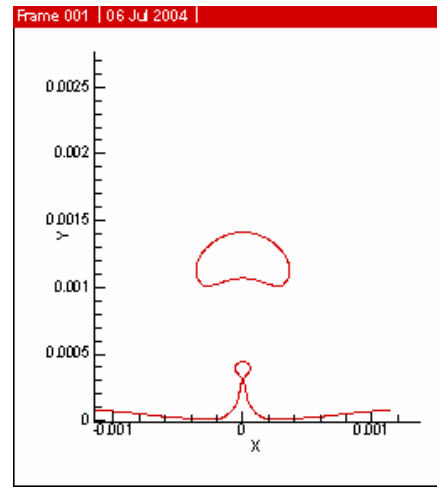
The wall model was chosen to be a constant heat flux one through a solid. The initial temperature field for the solid was taken to be at constant temperature with $\Delta T = 5 \text{ K}$, i.e. $T_{solid} = 651.15 \text{ K}$.

Bubble profile in the solution domain captured at various time-steps:

First half-cycle:

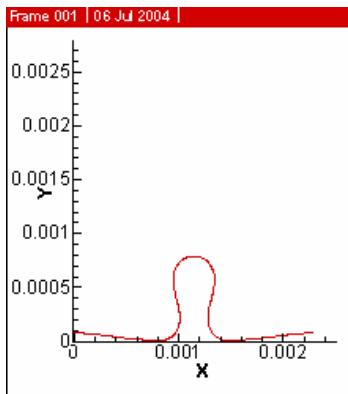


$t = 0.55s$

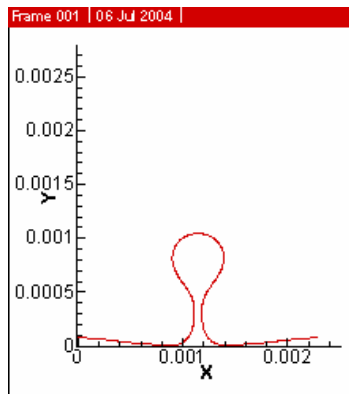


$t = 0.582s$

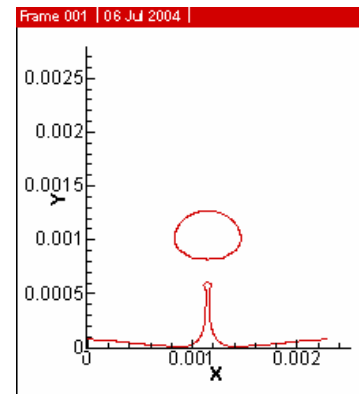
Second half-cycle:



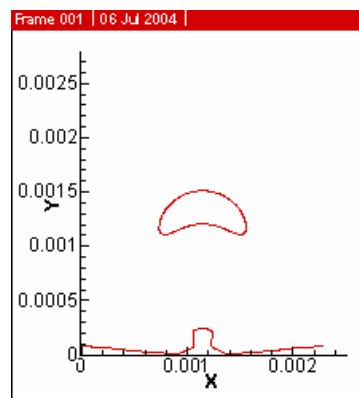
$t = 1.2255s$



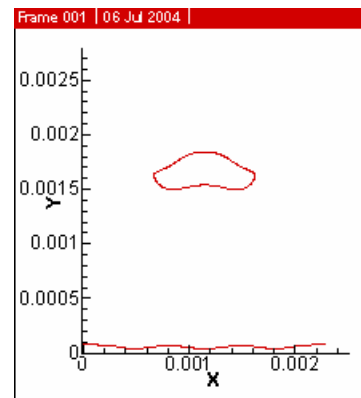
$t = 1.24s$



$t = 1.25s$



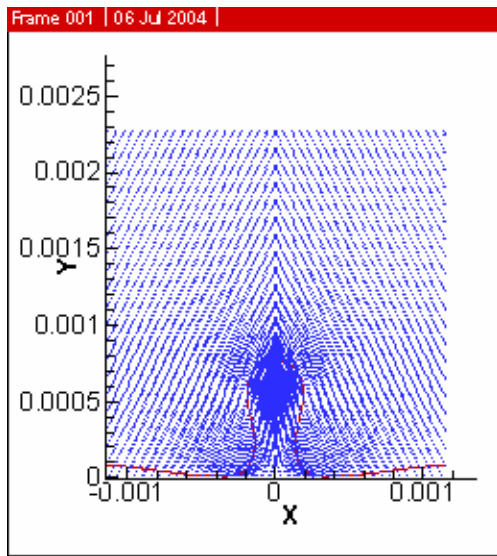
$t = 1.26s$



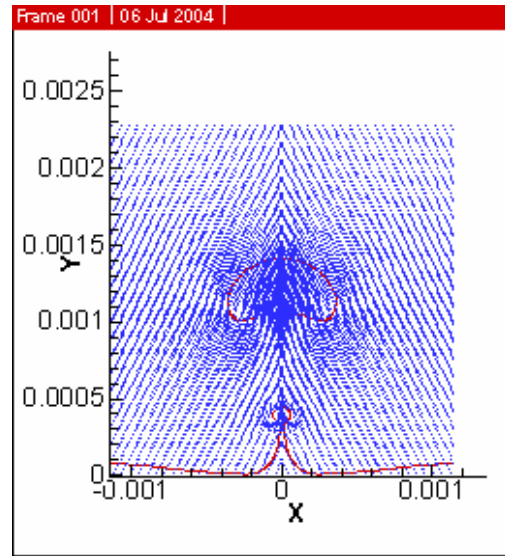
$t = 1.275s$

Velocity vector field at some time-steps:

First half-cycle:

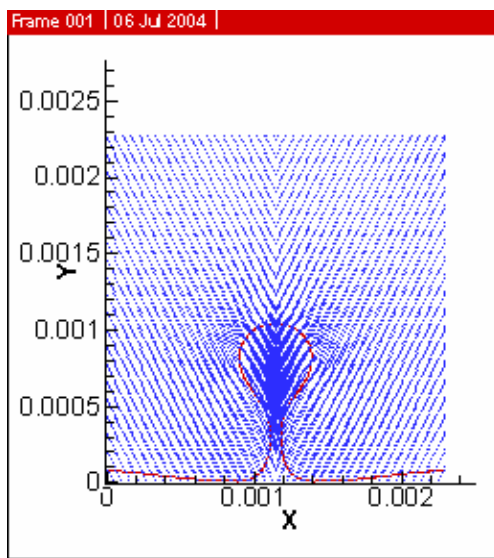


$t = 0.55\text{s}$

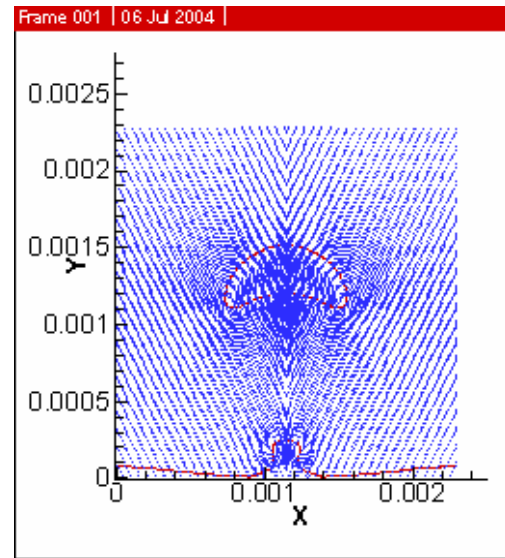


$t = 0.582\text{s}$

Second half-cycle:



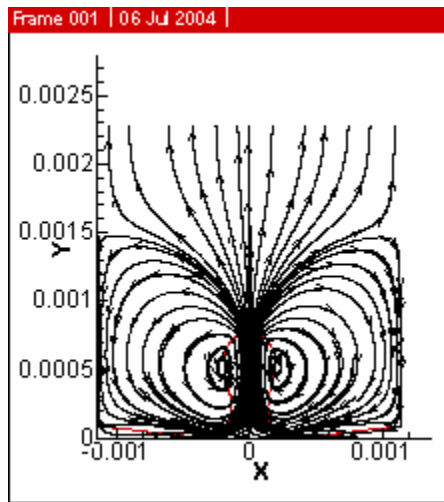
$t = 1.24\text{s}$



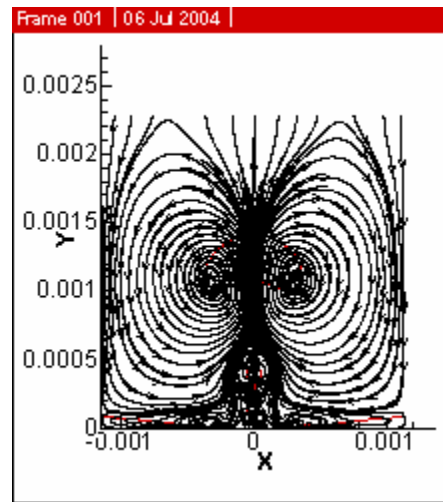
$t = 1.26\text{s}$

Streamlines at some time-steps:

First half-cycle:

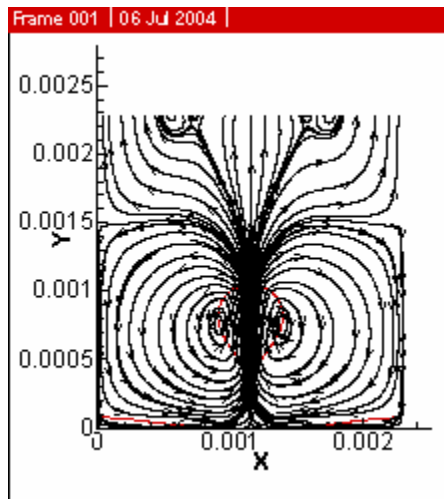


$t = 0.55$ s

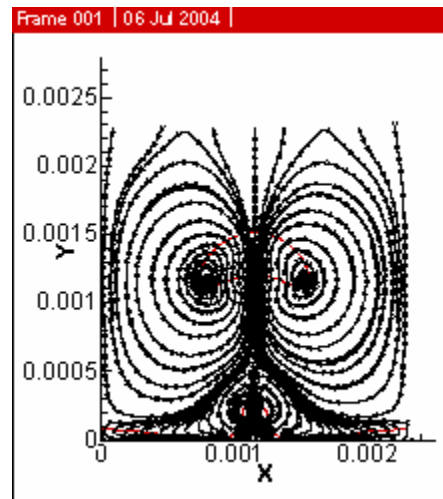


$t = 0.582$ s

Second half-cycle:



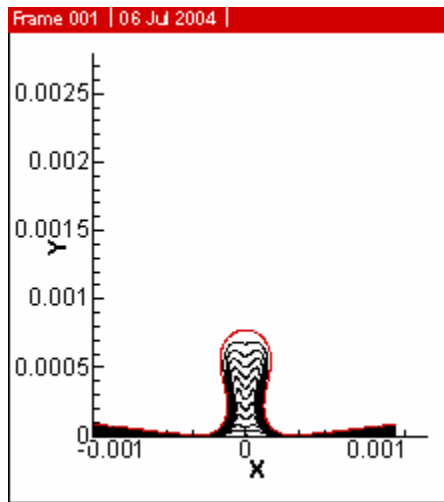
$t = 1.24$ s



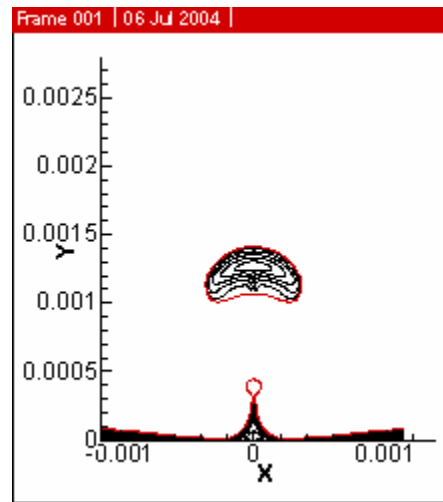
$t = 1.26$ s

Temperature contours at some time-steps:

First half-cycle:

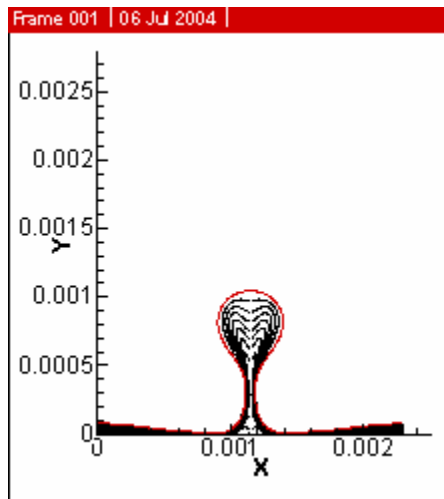


t = 0.55s

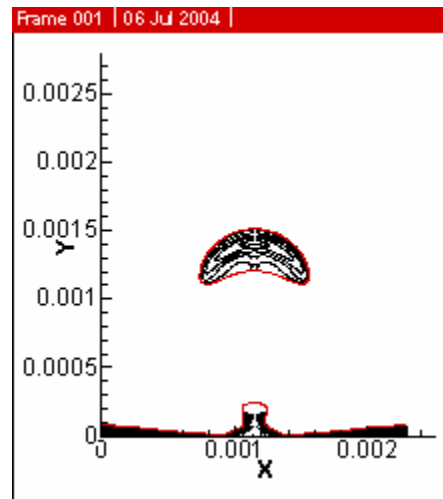


t = 0.582s

Second half-cycle:

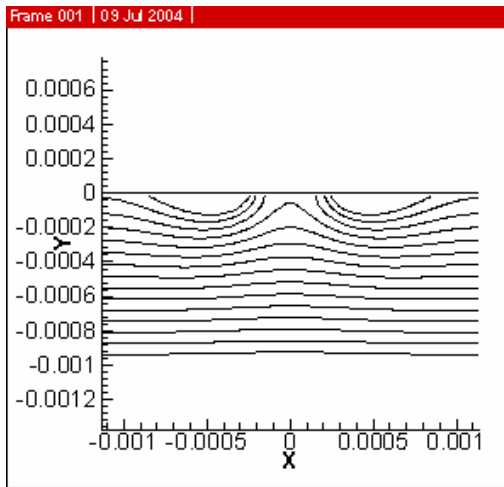


t = 1.24s

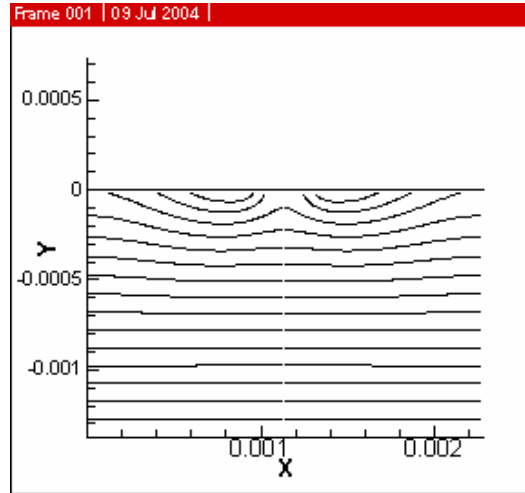


t = 1.26s

Temperature contours of the solid at some time-steps:

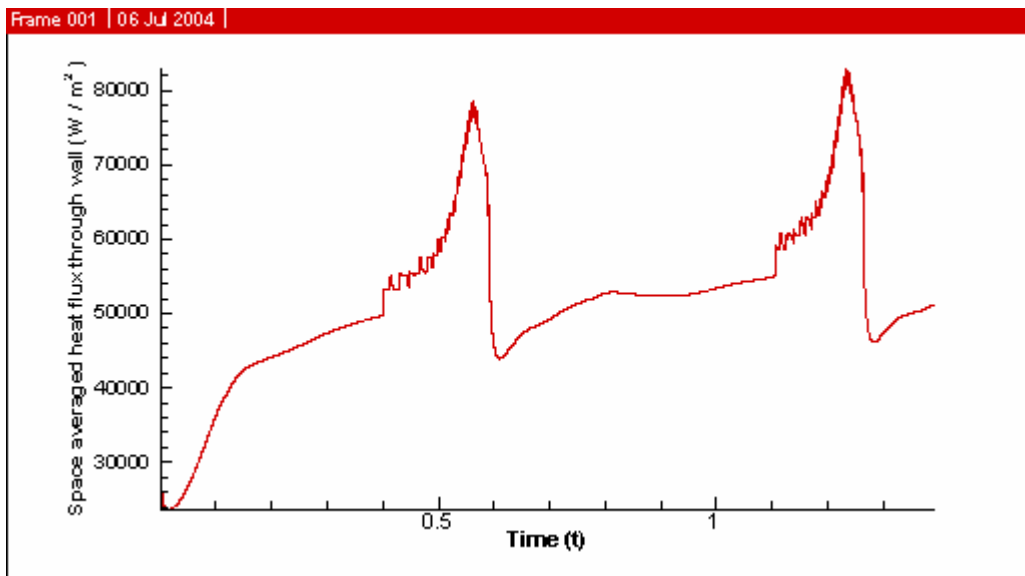


$t = 0.55\text{s}$

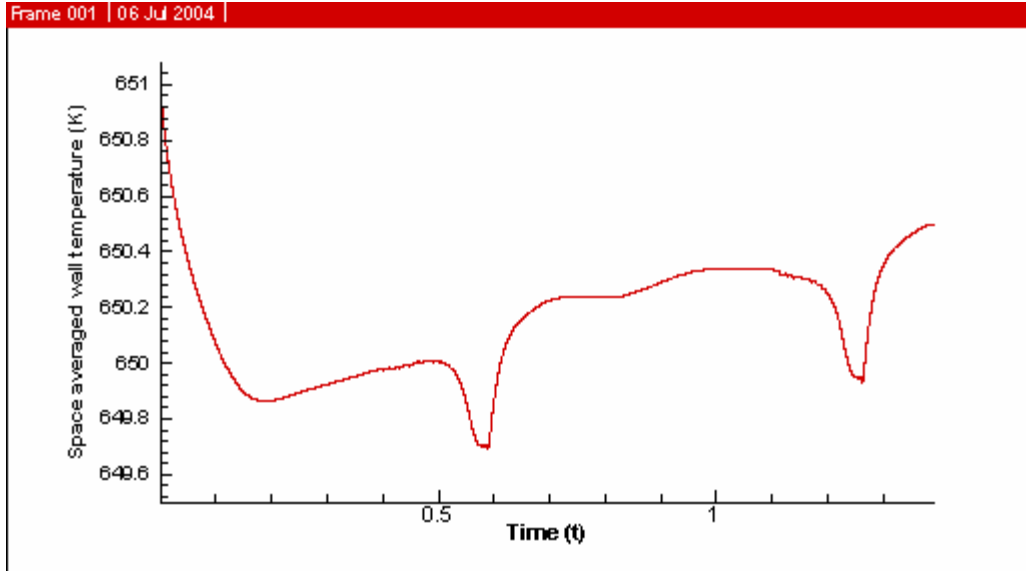


$t = 1.26\text{s}$

Space averaged heat flux through wall:



Space averaged wall temperature:



In this case apart from the time variation of space averaged heat flux through wall, the variation of space averaged wall temperature with time was also a rather interesting observation. Moreover the temperature contours of the solid region showed interesting patterns. Moreover this study has its importance in the fact that it is more close to the boiling phenomena that takes place in reality.

5.5. Case-5: Axisymmetric case :

The simulation performed by Agarwal *et al.* [17] was for a 2D case. Similar simulation has been performed here using CLSVOF techniques for an axisymmetric case. It is to be noted that the axisymmetric case being a mere approximation of the 3D case, can't manifest the periodic formation of bubble in a 3D space at nodes and antinodes. The only matter of interest in an axisymmetric case can be the formation of a single bubble. The fluid used is water at neat-critical point.

At the interface the following near-critical fluid properties are used:

$$T_{sat} = 646.15 \text{ K}; \quad P_{sat} = 94600 \text{ KPa}; \quad h_{lg} = 276.4 \times 10^4 \text{ KJ/Kg}; \quad \sigma = 0.07 \text{ mN/m}$$

The following properties are used for the liquid and vapour phase:

| | Density(ρ) (Kg/m ³) | Viscosity(μ) ($\mu\text{N s/m}^2$) | Conductivity(k) (mW/m K) | Specific Heat(c_p) (KJ/Kg K) |
|--------|---|---|---------------------------------|-------------------------------------|
| Liquid | 402.4 | 46.7 | 545.4 | 218.28 |
| Vapour | 242.7 | 32.38 | 538.3 | 352.27 |

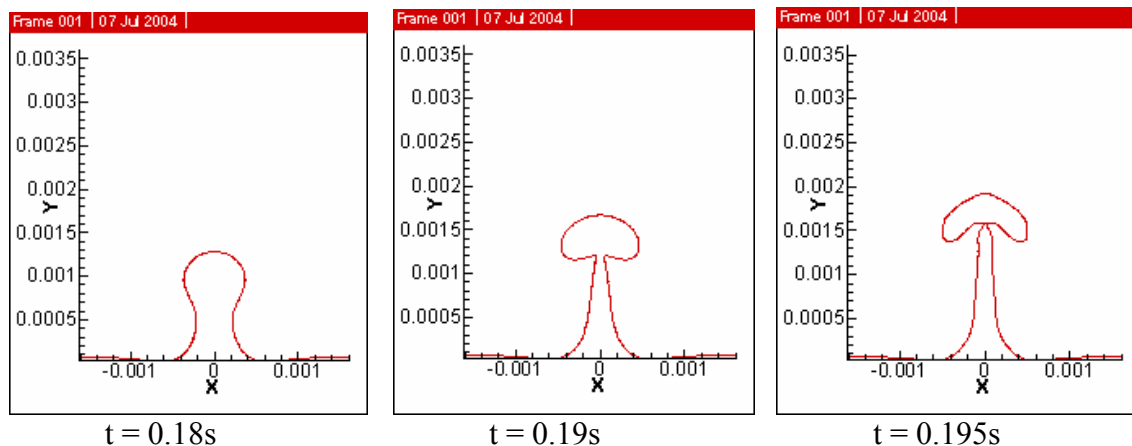
The fluid solution domain size is chosen to be $\frac{\lambda_0}{2\sqrt{2}} \times \lambda_0/\sqrt{2}$, i.e. $d = \lambda_0/\sqrt{2}$ and

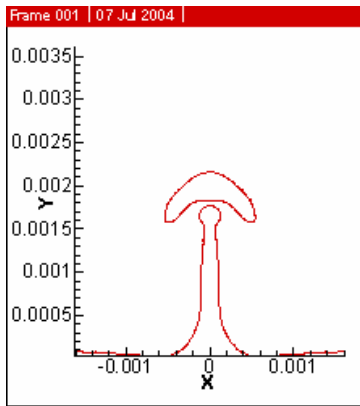
$H = \lambda_0/\sqrt{2}$. Grid resolution chosen was 100×200 . The grids were taken to be uniform square grids.

The solution was done for an axi-symmetric case.

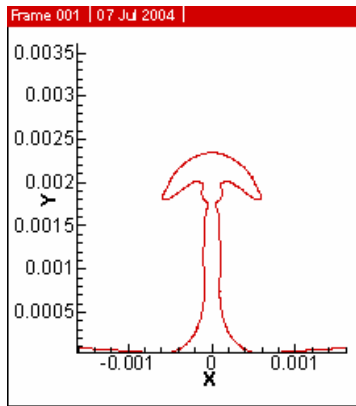
The wall model was chosen to be a constant temperature one with $\Delta T = 15 \text{ K}$, i.e. $T_{sup} = 661.15 \text{ K}$.

Bubble profile at various time-steps:

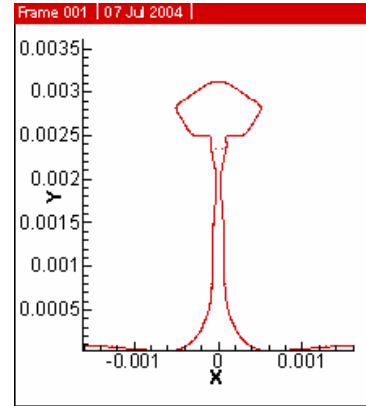




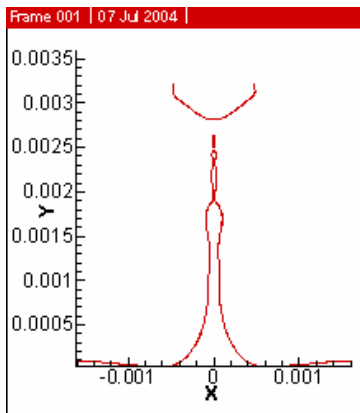
t = 0.2s



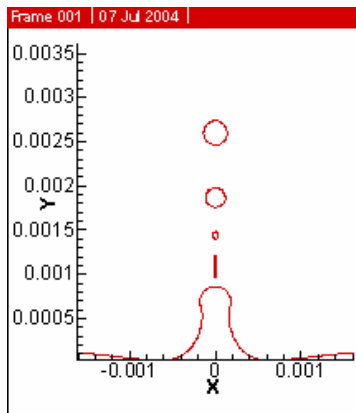
t = 0.205s



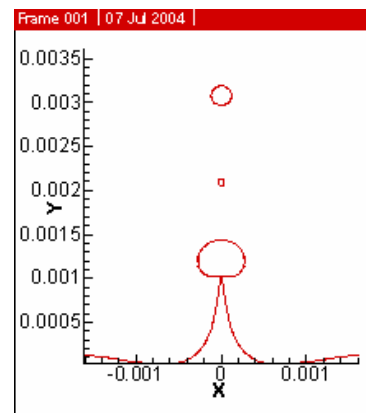
t = 0.22295s



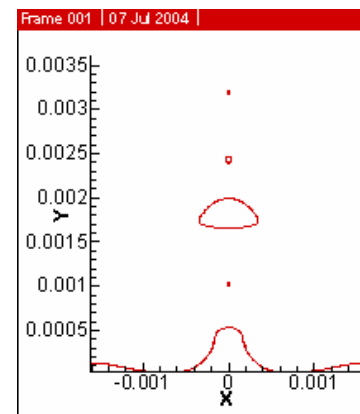
t = 0.23s



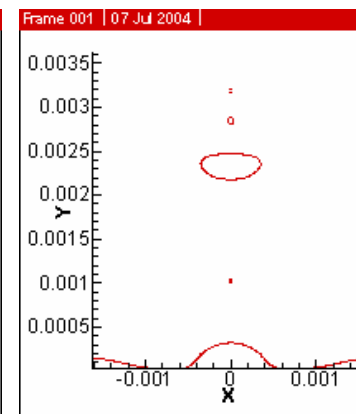
t = 0.25s



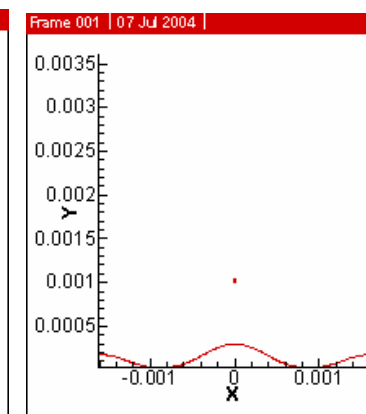
t = 0.275s



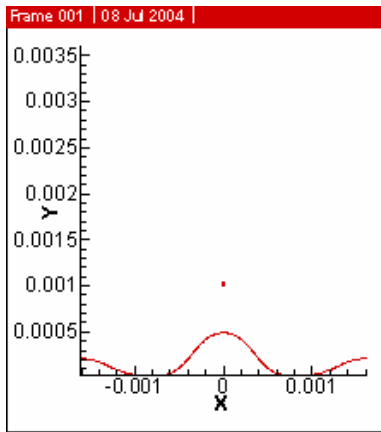
t = 0.2875s



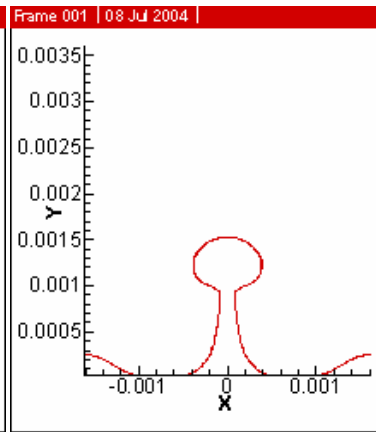
t = 0.3s



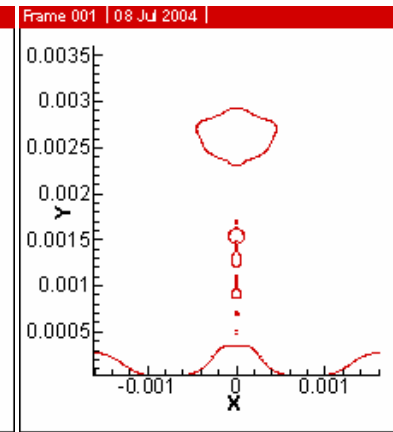
t = 0.35s



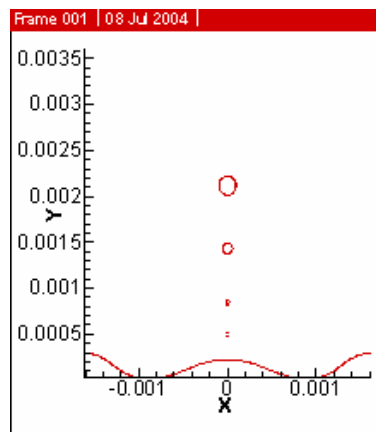
t = 0.4s



t = 0.45s

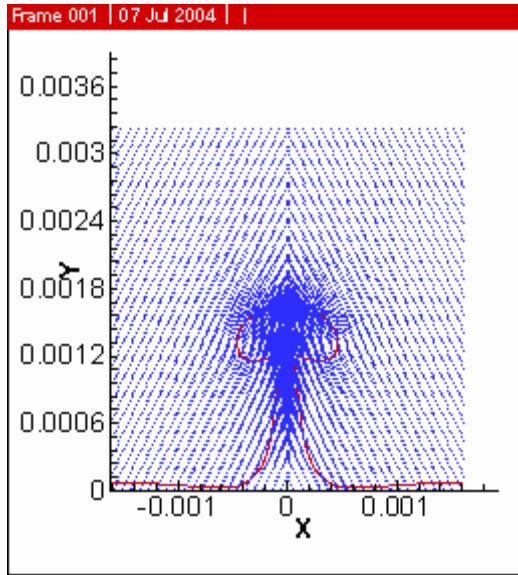


t = 0.482425s

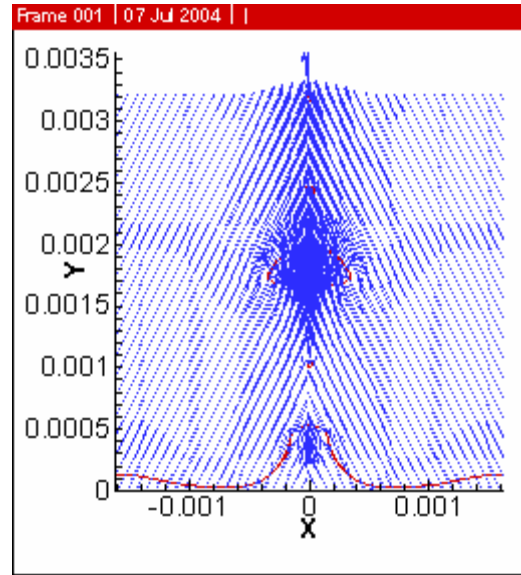


t = 0.5s

Velocity Vector field at some time-steps:

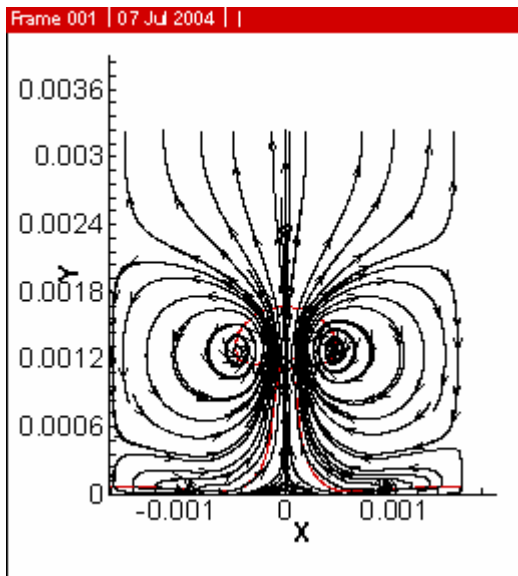


$t = 0.19\text{s}$

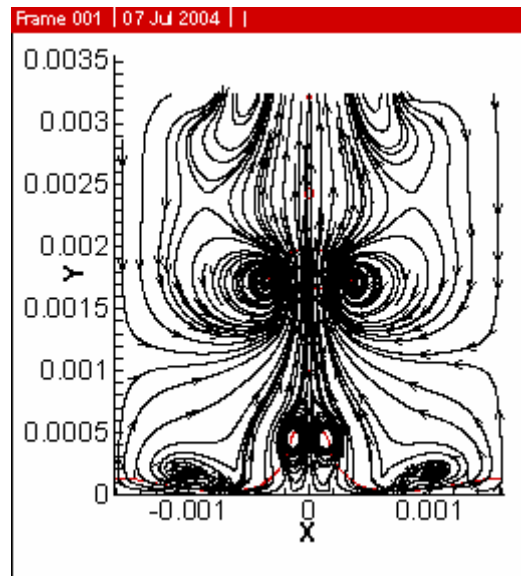


$t = 0.2875\text{s}$

Streamlines at some time-steps:

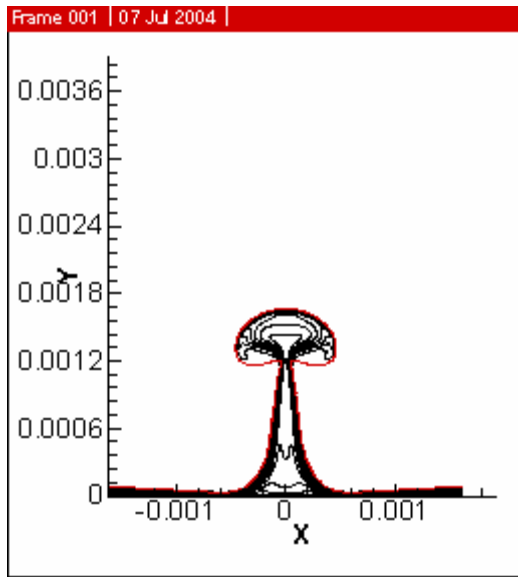


$t = 0.19\text{s}$

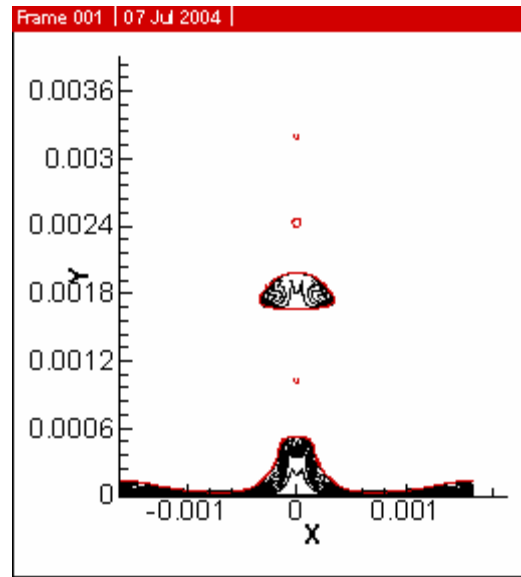


$t = 0.2875\text{s}$

Temperature contours at some time-steps:

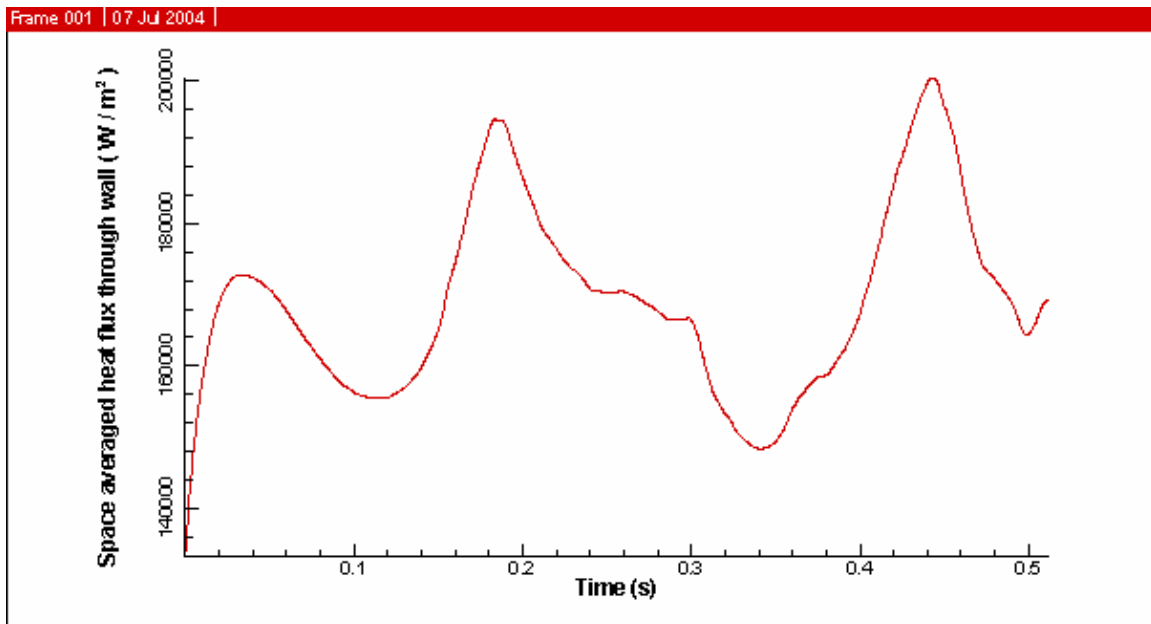


t = 0.19s



t = 0.2875s

Space-averaged heat flux through wall:



The axisymmetric case is rather an approximation to the 3D case of boiling. But in this case the formation of alternate bubble at nodes and antinodes can't be expected to observe. Rather if a bubble is formed at an antinode, it will represent a toroid-shaped structure rather than a bubble. Hence it is observed that the bubbles are formed at the same position in the solution domain.

An interesting phenomena can be observed at around $t=0.2s$ when the bubble once gets detached from the main stem and again gets rejoined with the stem. This phenomena may be attributed to the formation of comparatively long vapour stem than the 2D case. The formation of the elongated vapour stem reduces the surface tension forces. Hence the recoil speed of vapour stem due to the detachment of bubble is considerably reduced. As a result of which the reunion of bubble with the stem takes place.

6. References :

- [1] Code for film boiling written in FORTRAN 77.
- [2] P.J.Berenson, Film-Boiling Heat Transfer from a horizontal Surface, *J. Heat Transfer*, vol. 83, pp. 351-358, 1961.
- [3] M.Sussman and Elbridge Gerry Puckett, A Coupled Level Set and Volume-of-Fluid Method for Computing 3D and Axisymmetric Incompressible Two-Phase Flows, *J. Comput. Phys.* 162, 301-337 (2000).
- [4] Y.C.Chang, T.Y.Hou, B.Merriman and S.Osher, A Level Set Formulation of Eulerian Interface Capturing Methods for Incompressible Fluid Flows, *J. Comput. Phys.* 124, 449-464 (1996).
- [5] Hirt, C.W., and Nichols, B.D., 1981, Volume of Fluid (VOF) Method For the Dynamics of Free Boundary, *J. Comput. Phys.* 39, pp.201-225.
- [6] Samuel W.J. Welch and John Wilson, A Volume of Fluid Based Method for Fluid Flows with Phase Change, *J. Comput. Phys.* 160, 662-682 (2000).
- [7] Damir Juric and Gretar Tryggvason, Computations of Boiling Flows, *Int. J. Multiphase Flow*, vol. 24, pp. 387-410, 1998.
- [8] Salih Ozen Unverdi and Gretar Tryggvason, A Front-Tracking Method for Viscous, Incompressible, Multi-fluid Flows, *J. Comput. Phys.* 100, 25-37 (1992).
- [9] S.W.J.Welch, and T.Rachidi, Numerical Simulation of Film Boiling Including Conjugate Heat Transfer, *Numerical Heat Transfer, Part B*, 42, pp. 35-53, 2002.
- [10] G.Son and V.K.Dhir, Numerical simulation of Saturated Film Boiling on a Horizontal Surface, *J. Heat Transfer*, vol. 119, pp. 525-533, 1997.
- [11] D.Banerjee and V.K.Dhir, Study of Subcooled Film Boiling on a Horizontal Disc: Part I – Analysis, *J. Heat Transfer*, vol. 123, pp. 271-284, 2001.
- [12] V.K.Dhir, Numerical Simulation of Pool-Boiling Heat Transfer, *AIChE Journal*, vol. 47, pp. 813-834, 2001.
- [13] S.Oshe and J.A.Sethian, *J. Comput. Phys.* 79(1), 12 (1988).
- [14] Mark Sussman, Peter Smereka and Stanley Osher, A Level Set Approach for Computing Solutions to Incompressible Two-Phase Flows, *J. Comput. Phys.* 114, 146-159 (1994).
- [15] G.Son and V.K.Dhir, Numerical simulation of Film Boiling Near Critical Pressure With a Level Set Method, *J. Heat Transfer*, vol. 119, pp. 525-533, 1997.
- [16] J.U.Brackbill, D.B.Kothe and C.Zemach, A Continuum Method for Modeling Surface Tension, *J. Comput. Phys.* 100, 35-354 (1992).
- [17] D.K.Agarwal, S.W.J.Welch, G.Biswas, F.Durst, Planer Simulation of Bubble Growth in Film Boiling in Near-Critical Water Using a Variant of the VOF Method, *J. Heat Transfer*, vol. 126, pp. 1-11, 2004.